Neurobiology of Disease

Pronounced Hyperactivity, Cognitive Dysfunctions, and BDNF Dysregulation in Dopamine Transporter Knock-out Rats

Damiana Leo,[1] Ilya Sukhanov,[1,2] Francesca Zoratto,[3] Placido Illiano,[1] Lucia Caffino,[4] Fabrizio Sanna,[5] Giulia Messa,[4] Marco Emanuele,[1] Alessandro Esposito,[1] Mariia Dorofeikova,[2] Evgeny A. Budygin,[6,7] Liudmila Mus,[1,2] Evgenia V. Efimova,[7] Marco Niello,[1] Stefano Espinoza,[1] Tatyana D. Sotnikova,[7] Marius C. Hoener,[8] Giovanni Laviola,[3] Fabio Fumagalli,[4] Walter Adriani,[3] and Raul R. Gainetdinov[7,9]

[1]Fondazione Istituto Italiano di Tecnologia, Neuroscience and Brain Technologies Department Via Morego, 30 16163 Genoa, Italy, [2]Pavlov First Saint Petersburg State Medical University, Valdman Institute of Pharmacology, St. Petersburg, Russia, [3]Center for Behavioural Sciences and Mental Health, Istituto Superiore di Sanità, Viale Regina Elena, 299, I-00161 Roma, Italy, [4]Università degli Studi di Milano, Department of Pharmacological and Biomolecular Sciences, Via Balzaretti 9, 20133 Milan, Italy, [5]University of Cagliari, Department of Biomedical Sciences, Cittadella Universitaria, 09042 Monserrato (CA), Italy, [6]Department of Neurobiology and Anatomy, Wake Forest School of Medicine, Winston-Salem, North Carolina, [7]St. Petersburg State University, Institute of Translational Biomedicine, Universitetskaya Emb. 7-9, 199034 St. Petersburg, Russia, [8]Neuroscience Research, Roche Pharma Research and Early Development, Roche Innovation Center Basel, F. Hoffmann-La Roche Ltd., CH-4070 Basel, Switzerland, and [9]Skolkovo Institute of Science and Technology, 143025 Moscow, Russia

Dopamine (DA) controls many vital physiological functions and is critically involved in several neuropsychiatric disorders such as schizophrenia and attention deficit hyperactivity disorder. The major function of the plasma membrane dopamine transporter (DAT) is the rapid uptake of released DA into presynaptic nerve terminals leading to control of both the extracellular levels of DA and the intracellular stores of DA. Here, we present a newly developed strain of rats in which the gene encoding DAT knockout Rats (DAT-KO) has been disrupted by using zinc finger nuclease technology. Male and female DAT-KO rats develop normally but weigh less than heterozygote and wild-type rats and demonstrate pronounced spontaneous locomotor hyperactivity. While striatal extracellular DA lifetime and concentrations are significantly increased, the total tissue content of DA is markedly decreased demonstrating the key role of DAT in the control of DA neurotransmission. Hyperactivity of DAT-KO rats can be counteracted by amphetamine, methylphenidate, the partial Trace Amine-Associated Receptor 1 (TAAR1) agonist RO5203648 ((S)-4-(3,4-Dichloro-phenyl)-4,5-dihydro-oxazol-2-ylamine) and haloperidol. DAT-KO rats also demonstrate a deficit in working memory and sensorimotor gating tests, less propensity to develop obsessive behaviors and show strong dysregulation in frontostriatal BDNF function. DAT-KO rats could provide a novel translational model for human diseases involving aberrant DA function and/or mutations affecting DAT or related regulatory mechanisms.

Key words: ADHD; BDNF; dopamine; dopamine transporter; rat knock-out

---

Significance Statement

Here, we present a newly developed strain of rats in which the gene encoding the dopamine transporter (DAT) has been disrupted (Dopamine Transporter Knockout rats [DAT-KO rats]). DAT-KO rats display functional hyperdopaminergia accompanied by pronounced spontaneous locomotor hyperactivity. Hyperactivity of DAT-KO rats can be counteracted by amphetamine, methylphenidate, and a few other compounds exerting inhibitory action on dopamine-dependent hyperactivity. DAT-KO rats also demonstrate cognitive deficits in working memory and sensorimotor gating tests, less propensity to develop compulsive behaviors, and strong dysregulation in frontostriatal BDNF function. These observations highlight the key role of DAT in the control of brain dopaminergic transmission. DAT-KO rats could provide a novel translational model for human diseases involving aberrant dopamine functions.

Introduction

Dopaminergic innervations are prominent in the brain and the dopamine (DA) system exerts modulatory control of motivation, reward, cognition, and locomotion (Carlsson, 1987; Gainetdinov et al., 2008). Concentration of DA in the synaptic cleft is the primary determinant of DA signaling intensity. The key regulatory element of DA neurotransmission is DAT, belonging to a family of plasma membrane transporters of solute carrier family 6 (*SLC6*). DAT controls levels of extracellular DA and maintains DA stores by transporting released DA back into neurons. DAT is the well established target of many drugs of abuse and neurotoxins (Saunders et al., 2000; Kahlig et al., 2006; Wheeler et al., 2015; Siciliano et al., 2016). Amphetamine (AMPH) and cocaine (COC) are psychostimulants that are able to induce euphoria and hyperactivity by increasing extracellular DA via interaction with DAT.

The DAT-KO mouse model was generated >20 years ago by the groups of Marc Caron (Giros et al., 1996) and George Uhl (Sora et al., 1998). DAT-KO mice display a distinct behavioral phenotype: they are hyperactive, display certain cognitive deficits and show sleep dysregulation (Gainetdinov et al., 1999; Spielewoy et al., 2000). The hyperdopaminergic phenotype of DAT-KO mice has provided a simple model of hyperdopaminergic function in which the effects of various pharmacological agents affecting DA-related functions and behaviors have been evaluated. In particular, they are extremely sensitive to D2 dopamine receptor blockers and antipsychotics such as haloperidol and show a paradoxical inhibitory response to the psychostimulants AMPH and methylphenidate (MPH) (Gainetdinov et al., 1999; Spielewoy et al., 2000; Carboni et al., 2001).

DAT-KO mice have provided important information on the pathological consequences of aberrant DA function. DAT-KO mice are believed to best model attention deficit hyperactive disorder (ADHD) endophenotypes because they demonstrate spontaneous hyperactivity, deficits in cognitive tests, and antihyperkinetic responses to the psychostimulants used in ADHD treatments (Gainetdinov and Caron, 2000, 2001). At the same time, DAT-KO animals have provided numerous advances in understanding the pathology and pharmacology of other dopamine-related brain disorders such as schizophrenia (Gainetdinov et al., 2001; Wong et al., 2012, 2015), bipolar disorder

(Beaulieu et al., 2005), Parkinson's disease (Cyr et al., 2003; Sotnikova et al., 2005) and addiction (Rocha et al., 1998). Some patients diagnosed with ADHD, bipolar disorder and parkinsonism (Vaughan and Foster, 2013; Hansen et al., 2014) have rare coding variants of the SLC6A3 DAT gene. Recently, DAT-KO mice were used to evaluate the efficacy of adenoviral therapy for dopamine transporter deficiency syndrome (Illiano et al., 2017), a newly recognized parkinsonian-like condition with earlier hyperkinetic stage, the symptomatology of which is caused directly by an impaired DAT functioning due to loss-of-function mutations found in SLC6A3 DAT gene (Kurian et al., 2009, 2011; Ng et al., 2014; Yildiz et al., 2017).

Recent progress in the development of gene editing approaches has made it possible to perform such studies in genetically altered rats. Beyond obvious advantages of rat models, such as larger brain size for surgery and electrophysiological recordings and their closer physiological similarity to humans, rats have a much wider repertoire of well established behavioral approaches to investigate cognitive functions that are critical for modeling neuropsychiatric conditions.

Here, we present a new model of DAT deficiency, DAT-KO rats, generated by using zinc-finger nucleases (ZFN) technology (Geurts et al., 2009; Brown et al., 2013) used for the elimination of DAT gene. The current study describes detailed neurochemical, behavioral, and pharmacological characterization of this model that could open new perspectives in understanding pathology and pharmacology of human diseases involving aberrant DA function and/or mutations affecting DAT or DAT-related regulatory mechanisms.

Materials and Methods

Animals

ZFN design, construction, *in vitro* validation, microinjection, and founder selection were performed as described previously (Geurts et al., 2009; Carbery et al., 2010). The ZFN target site was as follows: CTCAT-CAACCCGCCACAGAcaccaGTGGAGGCTCAAGAG in the Exon 2 of Slc6a3 gene (NCBI Gene ID: 24898; Genomic NCBI Ref Seq: NC_005100.3; mRNA NCBI Ref Seq: NM_012694.2). The KO rat lines were created in the outbred Wistar–Han background at SAGE Labs. Adult littermate rats were housed by genotype in groups of three or four with *ad libitum* access to tap water and standard pellet food. They were kept at 22°C and on a 12/12 h light/dark cycle. All experiments were conducted in Istituto Italiano di Tecnologia (Genova, Italy), Università degli Studi di Milano (Milan, Italy), and Istituto Superiore di Sanità (Rome, Italy) with approved animal protocols in full compliance with the Italian Ministry of Health (DL 116/92; DL 111/ 94-B) and European Community (86/609/EEC) directives regulating animal research. All efforts were made to minimize animal suffering and to reduce the number of animals used. Rats of both sexes were used in all experiments excluding behavioral cognitive tests, in which only males were used .

Genotyping was performed by PCR followed by enzymatic digestion with BtsI MutI (New England Biolabs).

Real-time PCR

Animals were killed and prefrontal cortex (PFC), dorsolateral striatum (DLStr), and midbrain were dissected and dissociated for 15 min at 37°C with Pronase enzyme (Sigma-Aldrich) in Hank's balanced salt solution (HBSS; Invitrogen). Brain samples were triturated with 3 glass pipettes of decreasing tip diameter and centrifuged at 900 rpm at room temperature for 5 min. To remove excess debris, cell pellets were resuspended in HBSS and filtered through a 70 μm mesh (BD Falcon, catalog #352350). Cells-to-CT kit (Life Technology) was used to produce DNase I digested cell lysates and perform cDNA synthesis according to the manufacturer's instructions. cDNAs were used for TaqMan singleplex PCR. To prevent false-positives originating from genomic DNA, we used negative control samples without reverse transcriptase. All reagents were supplied by Applied Biosystems. PCR master mix contained 1× TaqMan Universal

PCR Master Mix, 1× Gene Expression Assay mix, and 1 μl of cDNA for a total volume of 20 μl. The following Gene Expression Assays were used: Drd2 (Assay ID Rn01452984_m1), Drd1a (Assay ID Rn00569454_m1), TH Assay ID Rn00562500_m1); Gapdh (Assay ID Rn01775763_g1), and Hprt (Assay ID Rn01527840_m1). Samples were run in three replicates for each Gene Expression Assay. PCRs were performed on a 7900 Thermal Cycler (Applied Biosystems) with 40 cycles of 95°C for 15 s and 60°C for 1 min. CT values for each gene were normalized to CT values for GAPDH and HPRT to obtain a relative expression level for each replicate and the three replicates were averaged together.

For BDNF analysis, an aliquot of total RNA of each sample ($n = 5$ WT and $n = 5$ DAT-KO rats) was treated with DNase to avoid DNA contamination. RNA was analyzed by a TaqMan qRT-PCR instrument (CFX384 real-time system; Bio-Rad Laboratories) using the iScriptTM one-step RT-PCR kit for probes (Bio-Rad Laboratories). Samples were run in 384-well formats in triplicate as multiplexed reactions. Data were analyzed with the comparative threshold cycle ($\Delta\Delta$Ct) method using 36B4 as a reference gene. The primer efficiencies were experimentally set up for each pair of primers.

Probes and primers for total BDNF, cAMP responsive element binding protein (Creb), calcium-responsive factor (CaRF), Neuronal PAS Domain Protein 4 (Npas4) and 36B4 were purchased from Eurofins MWG-Operon and their sequences were as follows: total BDNF: forward primer 5′-AAGTCTGCATTACATTCCTCGA-3′, reverse primer 5′-GTTTTCTGAAAGAGGGACAGTTTAT-3′, probe 5′-TGTGGTTTGT TGCCGTTGCCAAG-3′; Creb: forward primer 5′-AGATTCTAGTG CCCAGCAAC-3′, reverse primer 5′-CTGTGCGAATCTGGTAT GTTTG-3′, probe 5′-TGTTCAAGCTGCCTCTGGTGATGT-3′; Npas4: forward primer 5′-TCATTGACCCTGCTGACCAT-3′, reverse primer 5′-AAGCACCAGTTTGTTGCCTG-3′, probe 5′-TGATCGCCTTT TCCGTTGTC-3′; CaRF: forward primer 5′-GAGATGCACACACC ATTCCA-3′, reverse primer 5′-GTGTTGGCTCATTGGGTTCT-3′, probe 5′-CAGCCATCCAGCTCTTGTTGAAGA-3′; and 36B4: forward primer 5′-TTCCCACTGGCTGAAAAGGT-3′, reverse primer 5′-CGCAGCCGCAAATGC-3′, probe 5′-AAGGCCTTCCTGGCCGATC-CATC-3′.

Probes and primers for BDNF exon IV and BDNF exon VI were purchased from Life Technologies (BDNF exon IV: ID Rn01484927_m1 and BDNF exon VI: ID Rn01484928_m1). Thermal cycling was started with 10 min incubation at 50°C (RNA retrotranscription) then 5 min at 95°C (TaqMan polymerase activation). After this, 39 PCR cycles were run. Each PCR cycle consisted of heating the samples at 95°C for 10 s to enable the melting process and then for 30 s at 60°C for the annealing and extension reaction.

Protein extraction and Western blotting

Protein extraction and preparation of samples for Western blot analysis were performed as described previously (Vecchio et al., 2014). Briefly, the tissues were dissected from freshly harvested brains. Brain samples were mechanically homogenized in RIPA buffer (50 mmol/L Tris-HCl, pH 7.4, 150 mmol/L NaCl/1% Nonidet P-40/0.5% sodium deoxycholate/0.1% SDS; Sigma-Aldrich) plus protease inhibitor mixture (Roche, catalog #1873580), and protein concentration was measured using a BCA protein assay kit (Thermo Scientific). Protein extracts (25 μg) were separated by 10% SDS/PAGE and transferred to nitrocellulose membranes (GE Healthcare). Blots were immunostained overnight at 4°C with the following primary antibodies: Gapdh (FL-335; sc-25778; Santa Cruz Biotechnology) and DAT (C-20; sc-1433; Santa Cruz Biotechnology). After washing, the membranes were incubated for 2 h at room temperature with the appropriate secondary antibody (anti-mouse, anti-rabbit, or anti-rat). After secondary antibody incubations, membranes were washed and finally incubated with ECL detection reagent (GE Healthcare, catalog #RPN2232) for 5 min.

For BDNF analysis, the medial PFC was dissected from a 2 mm section extending from approximately bregma +5.16 to +3.24 (Paxinos and Watson, 2005) and DLStr was dissected from a 2 mm section immediately caudal to the PFC section from $n = 5$ WT and $n = 5$ DAT-KO rats. Brain areas were immediately frozen on dry ice and stored at −80°C until being processed for molecular analysis. Protein extraction was per-

formed as described previously (Caffino et al., 2017) with minor modifications. Briefly, PFC and DLStr were homogenized in a Teflon-glass potter in cold 0.32 M sucrose buffer, pH 7.4, containing 1 mM HEPES, 0.1 mM EGTA, and 0.1 mM PMSF in the presence of commercial mixtures of protease (Roche) and phosphatase (Sigma-Aldrich) inhibitors and then sonicated. The homogenate of DLStr was centrifuged at 800 g for 5 min and the obtained supernatant was centrifuged at 13,000 × g for 15 min, obtaining a pellet (P2) and a supernatant (S2), referred as the cytosolic fraction. The P2 pellet was resuspended in buffer containing 150 mM KCl and 1% Triton X-100 and centrifuged at 100,000 × g for 1 h. The resulting supernatant, referred as the Triton X-100-soluble fraction, was stored at −20°C; the pellet, referred as PSD or the Triton X-100-insoluble fraction, was homogenized in a glass–glass potter in 20 mM HEPES with protease and phosphatase inhibitors and stored at −20°C in presence of 30% glycerol. Total protein content was measured according to the Bradford Protein Assay procedure (Bio-Rad) using bovine serum albumin as calibration standard. Equal amounts of protein were run under reducing conditions on the criterion TGX precast gels (Bio-Rad Laboratories) and then electrophoretically transferred onto nitrocellulose membranes (Bio-Rad). Blots were blocked 1 h at room temperature with 10% nonfat dry milk in TBS + 0.1% Tween 20 buffer, incubated with antibodies against the phosphorylated forms of the proteins, and then stripped and reprobed with the antibodies against corresponding total proteins. The conditions of the primary antibodies were the following: the mature form of BDNF (mBDNF) (1:1000; Icosagen); anti-phospho trkB Y706 (1:1000; Santa Cruz Biotechnology); anti-total trkB (1:750; Santa Cruz Biotechnology); anti-phospho CaMKII T286 (1:2000; Thermo Scientific); anti total CaMKII (1:5000; Millipore Bioscience Research Reagents); anti-total PSD95 (1:4000; Cell Signaling Technology), and anti-β-Actin (1:10000; Sigma-Aldrich). Results were standardized using β-actin as the control protein, which was detected by evaluating the band density at 43 kDa. Immunocomplexes were visualized by chemiluminescence using the Chemidoc MP Imaging System (Bio-Rad Laboratories) and analyzed using Image Lab software from Bio-Rad Laboratories. The activations of the proteins investigated were expressed as a ratio between the phosphorylated and the respective total forms.

In vivo *microdialysis*

In vivo brain microdialysis was performed in the right dorsal striatum (DStr) of freely moving rats (Carboni et al., 2001; Budygin et al., 2004) using concentric microdialysis probes (2 mm membrane length cutoff 6000 Da; CMA-11; CMA/Microdialysis). Stereotaxic coordinates for the position of the probes were chosen according to the atlas of Paxinos and Watson (2005) and are relative to the bregma: AP 1.0, L 3.0, DV −6.6. Before fixation in the stereotaxic apparatus, the animals were anesthetized with an oxygen/isoflurane mixture. The probes were implanted in the brain vertically through a small drilled aperture in the scull and fixed with dental cement. During implantation into the brain and for 1 h afterward, the dialysis probes were perfused with artificial CSF (aCSF) containing the following (in mM): 147 NaCl, 2.7 KCl, 1.2 CaCl$_2$, and 0.85 MgCl$_2$ (CMA Microdialysis). One hour after the operation, the animals were returned to their home cages.

Approximately 24 h after surgery, the dialysis probes were connected to a syringe pump and perfused with the aCSF at 1.0 μl/min for 60 min (equilibration period). To determine the basal extracellular DA levels reliably in the striatum of freely moving rats, a quantitative "low perfusion" rate microdialysis experiment was conducted (Gainetdinov et al., 2003). The perfusate was collected at a perfusion rate of 0.1 μl/min every 90 min over a 6 h period into collection tubes containing 2 μl of 1 M perchloric acid. To determine the effect of AMPH (3 mg/kg, i.p.) on the extracellular DA level, a "conventional" microdialysis approach was used. Dialysis probes were connected to a syringe pump and perfused with aCSF at 1 μl/min for at least 60 min for equilibration. Then perfusate was collected every 20 min for 1 h before injection and 2 h after injection of AMPH.

HPLC

HPLC measurements were performed as described previously (Leo et al., 2014). Brain tissues were dissected from WT, KO, and heterozygous

(HET) rats and homogenized in 40 volumes of 0.1 M HClO$_4$. After centrifugation and filtration, the samples were analyzed by HPLC as described below. The protocol for sample preparation for the HPLC determination of tissue monoamines and their metabolites was performed as described previously. Measurements of DA, 5-hydroxytryptamine (5-HT) and metabolites in tissue samples and DA in microdialysis samples were performed by HPLC with electrochemical detection (ALEXYS LC-EC system; Antec Leyden) with a 0.7 mm glass carbon electrode (VT-03; Antec Leyden). The system was equipped with a reverse-phase column (3 μm particles, ALB-215 C18, 1 $\times$ 150 mm; Antec Leyden) at a flow rate of 200 μl/min. The mobile phase contained 50 mM H$_3$PO$_4$, 50 mM citric acid, 8 mM KCl, 0.1 mM EDTA, 400 mg/L octanesulfonic acid sodium salt, and 10% (v/v) methanol, pH 3.9. The sensitivity of this method permitted the detection of fmol DA. Dialyzate samples (11 μl) were injected into HPLC without any additional purification.

Fast-scan cyclic voltammetry (FSCV)
The brains were sectioned in cold carboxygenated aCSF containing the following (in mM): 126 NaCl, 2.5 KCl, 1.2 NaH$_2$PO$_4$, 25 NaHCO$_3$, 2.4 CaCl$_2$, 11 D-glucose, and 1.2 MgCl$_2$, on a VT1000S vibrating microtome (Leica Microsystems) at a thickness of 300 μm. Coronal slices containing the DStr were allowed to recover for at least 1 h at room temperature in carboxygenated aCSF. For recordings, slices were superfused with 32°C carboxygenated aCSF at a flow rate of 1 ml/min. FSCV recordings started 20 min after transfer to the slice chamber. Carbon fiber electrodes (7 μm diameter; Goodfellow) were made as described previously (Kuhr and Wightman, 1986; Kawagoe et al., 1993). The carbon fibers were trimmed with a scalpel to 80–120 μm under a microscope (Nikon) A carbon fiber microelectrode was inserted into the slice and a twisted bipolar stimulating electrode (Plastics One) was placed on the surface of the brain slice ~200 μm away. The potential of the working electrode was held at −0.4 V and scanned to +1.3 V and back at 300 V/s. Axonal DA release in the striatum was evoked by a single biphasic electrical pulse (1 ms long, 400 μA) every 2 min through a stimulus isolator (AM Systems). Data were filtered to reduce noise. Oxidation and reduction peaks were observed at ~ +0.65 V and −0.2 V (vs Ag/AgCl reference) identifying DA as the released chemical. Electrodes were calibrated in a flow injection system using 1 μM DA (Sigma-Aldrich).

FSCV kinetic analysis. There were several established criteria for choosing which DA signals to use for analysis, two of these being that there should be no confounding electrical artifacts to interfere with the DA traces and no pH shifts during recordings, which allow for a flat baseline before stimulation and provide the most uncontaminated DA dynamics as possible. Next, a 10:1 signal-to-noise ratio was used to guarantee that the actual signal was separated from background. All of these criteria insured accuracy in analysis. One to two recordings from each experimental group were excluded from analysis based on these criteria.

Data analysis was performed using Demon voltammetry software described (Yorgason et al., 2011). Briefly, computations were based on user-defined positions on current traces for baseline (Pre-Stim cursor), peak (Peak Cursor), and return to baseline (Post-Stim cursor) positions. Half-life values were determined from exponential fit curves based on Peak cursor and Post-Stim cursor positions using a least-squares constrained exponential fit algorithm (National Instruments) (Yorgason et al., 2011a). These measurements were performed on individual traces within each experiment. These numbers were then averaged within each experimental group (WT, KO, and KO treated) and reported as mean ± SEM. Half-life is considered to be a reliable measure for evaluating changes in striatal DA clearance *in vivo* and *in vitro*. This parameter accurately distinguishes differences in clearance rate similar to other established measures (Yorgason et al., 2011).

Locomotor activity in a novel environment
Locomotor activity was evaluated as described previously (Sukhanov et al., 2014) using an automated Omnitech Digiscan apparatus (AccuScan Instruments) under illuminated conditions. The apparatus included four open field monitors, each consisting of a set of 16 light beams arrayed in the horizontal $\times$ and *y*-axes. The hardware detected beams broken by the animal, allowing the software to determine the location of the rat in the

cage. Cages were divided into four compartments (20 $\times$ 20 cm). Animals were tested individually for defined periods with 5 min intervals. The total distance traveled was measured and expressed in terms of centimeters traveled by the animal. In addition, vertical activity as expressed in terms of the number of beam breaks. All rats were habituated to the test room for at least 1 h before testing. Effects of drugs on locomotor activity in a novel environment were tested 30 min after placement of animals into locomotor activity monitor. D-AMPH hydrochloride, MPH hydrochloride, haloperidol (Sigma-Aldrich), and RO5203648 (F. Hoffmann-La Roche) were dissolved as described previously (Gainetdinov et al., 1999; Spielewoy et al., 2000; Revel et al., 2012). For all behavioral experiments, drugs were administered intraperitoneally in a volume of 1 ml/kg. All solutions were made fresh daily.

Twenty-four-hour spontaneous locomotor activity in a home cage
Rats were monitored continuously for spontaneous home cage locomotor activity by means of an automatic device equipped with small passive infrared sensors placed on a standard rack over the top of each home-cage (ActiviScope system; TechnoSmart). These sensors (20 Hz) detected any movement of rats: scores were automatically divided into 60 min intervals.

Y-maze spontaneous alternation test
To measure spontaneous alternation behavior and exploratory activity, a white plastic material Y-maze with arms 40 cm (long) by 6 cm (wide) with 13 cm walls was used. Each animal was tested in a single 8 min session, during which the animal was placed in the central platform and allowed free exploration of the maze. Spontaneous alternation, expressed as a percentage, refers to ratio of arm choices differing from the previous two choices to the total number of arm entries.

Schedule-induced polydipsia
Apparatus. The experiments were performed in five standard operant conditioning chambers for rats, with interior dimensions 31 cm $\times$ 27 cm $\times$ 33 cm located in sound-attenuating and light-proof cubicles. Each cubicle was equipped with an electric fan that provided background white noise during the experimental sessions. The right wall of each chamber contained three metal panels with built-in appliances. Each chamber was illuminated by houselights (25 W) installed at the top of the central panel was turned on during experiments. The pellets tray was situated 2 cm from floor also at the central panel. A water bottle was fitted at the right panel such a way that the drinking spout of the bottle was obtainable for rats ~3 cm from the floor. The chamber inputs were connected to the operating PC equipped with Med-PC software through the MED interface (MED Associates). The volume of water consumed during each session was measured by weighing the bottle at the start and at the end of the session.

Polydipsia induced by fixed-time 60 s schedule of reinforcement. Rats were habituated to the operant chambers and to pellet feeding within daily magazine training sessions. During the sessions, the rats were placed in the chambers with 15 pellets in the food trough for 30 min. The next day after successful magazine training (all animals had eaten all pellets), the rats were given daily 1 h sessions (6 d a week) with fixed-time 60 s (FT 60 s) schedule of food reinforcement (i.e., food pellets were delivered every 60 s independently of an animal's behavior). Within the experimental sessions the rats had *ad libitum* access to the drinking spouts of the bottles filled with fresh tap water. When the rats had acquired stable adjunctive drinking behavior (i.e., the volume of consumed water did not change >10% within two consecutive days), three test sessions were performed. During each test session, the volume of consumed water was assessed.

Startle and prepulse inhibition (PPI) test
Startle and PPI testing were performed as described previously (Farné, 1970; Frau et al., 2016). The apparatus used for detection of startle reflexes (Med Associates) consists of four standard cages placed in sound-attenuated chambers with fan ventilation. Each cage consists of a Plexiglas cylinder of 9 cm diameter mounted on a piezoelectric accelerometric platform connected to an analog–digital converter. Two separate speakers convey background noise and acoustic bursts. Both speakers and startle cages are connected to a main PC, which detects and analyzes
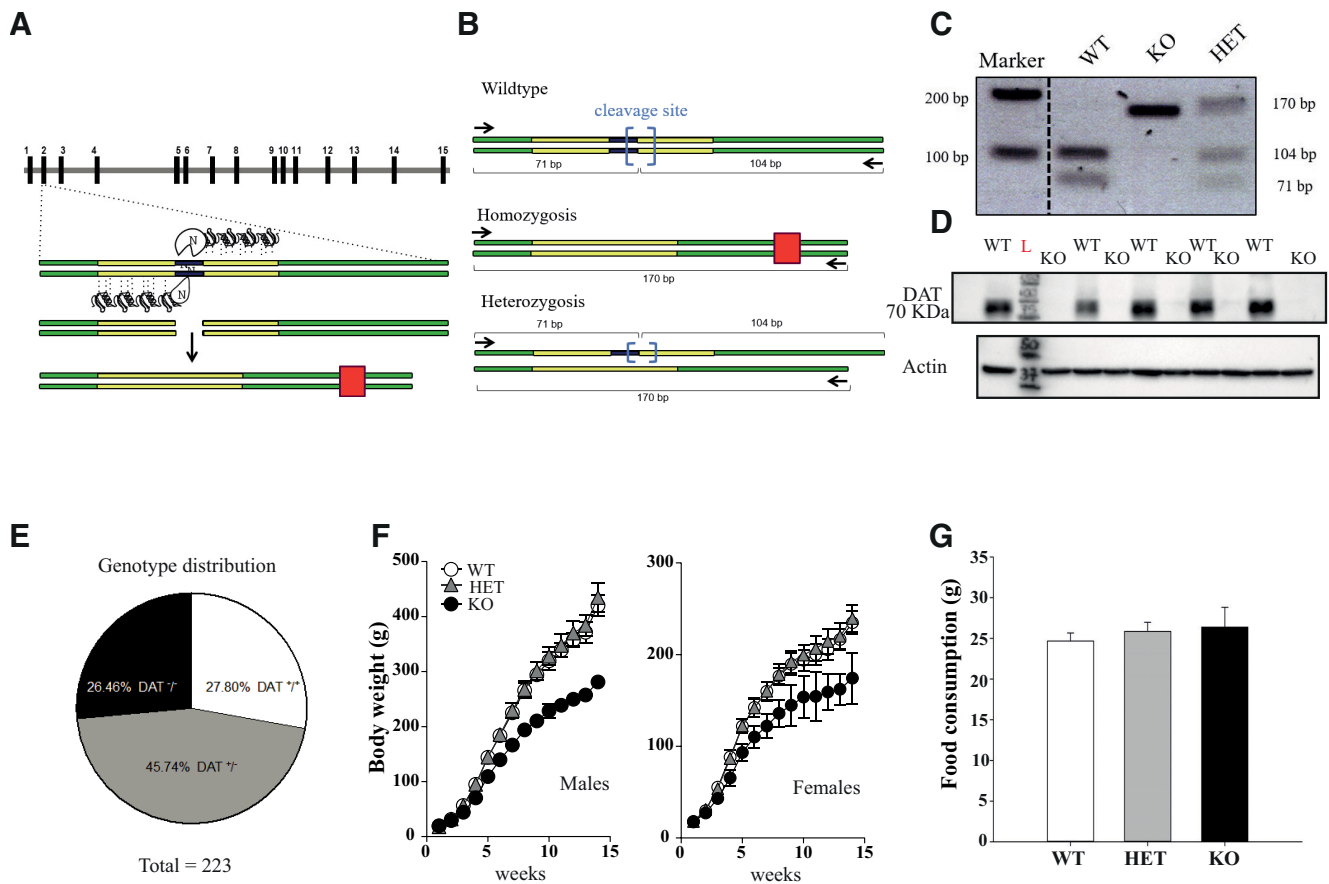
Figure 1. Generation of DAT KO (KO) rats. **A**, DAT-KO rats were generated by using ZFN technology that produces a 5 bp deletion and an early stop codon. Green solid lines indicate exons 2 and 3, gray solid lines indicate introns; yellow boxes indicate DNA domains interaction sites; blue box indicates KO targeting site; red box indicates early stop codon generated after frameshift due to cleavage of 5 bp operated by ZFN. **B**, **C**, PCR primers were designed (black arrows). WT DNA contains BtsIMutI restriction enzyme site (blue brackets). WT-amplified DNA is fully digested into two low-molecular-weight bands (104 and 71 bp). Homozygote-mutated DNA loses digestion sites on both alleles, therefore resulting in only one final PCR product of 170 bp. Heterozygosis shows both digested DNA at lower molecular weight from the WT allele and mutated DNA at 170 bp. **D**, Western blot analysis of DAT expression in striatal samples of WT and DAT-KO rats. DAT-KO rats, in contrast to WT controls, show complete absence of DAT protein expression. Another representative blot is shown in Figure 1-1 available at https://doi.org/10.1523/JNEUROSCI.1931-17.2018.f1-1. **E**, Rats were bred following a HET–HET female breeding scheme. A total of 223 animals were born from 19 offspring and we obtained 62 DAT $^{+/+}$ (26.46%), 102 DAT $^{+/-}$ (45.74%), and 59 DAT $^{-/-}$ (27.80%), numbers very close to the ratio (1:2:1) expected in the absence of prenatal and postnatal death. Infantile mortality was completely absent for all 3 genotypes followed for up to 4 months. **F**, Developmental phenotype. Both DAT-KO male and female rats develop normally but have lower weight compared with DAT-HET and WT rats ($n = 10$–20 per group). **G**, Analysis of food consumption for 3 d (*ad libitum*) revealed no difference between genotypes (males, $n = 6$–8 per genotype).

all chamber variables with specific software. Before each testing session, acoustic stimuli and mechanical responses were calibrated.

The test begins with a 5 min acclimatization period with a 70 dB background white noise, which continues for the entire session. The acclimatization period is followed by three blocks, each consisting of a sequence of trials: the first and the third block consist of five pulse-alone trials of 115 dB. The second block consists of a pseudorandom sequence of 50 trials, including 12 pulse-alone trials; 30 trials of pulse preceded by 74, 78, or 82 dB prepulses (10 for each level of prepulse loudness); and 8 no-pulse trials in which only the background noise is delivered. Intertrial intervals (i.e., the time between two consecutive trials) were selected randomly between 10 and 15 s. The percentage PPI was calculated using the following formula: $100 -$ (mean startle amplitude for prepulse pulse trials/mean startle amplitude for pulse alone trials) $\times$ 100.

Experimental design and statistical analysis
All data are expressed as the mean $\pm$ SEM and the statistical analysis was performed with SPSS 21.0, SigmaPlot 12.5, and GraphPad Prism 6 software. Sample sizes were determined by intrinsic variation of dataset. All sample sizes are indicated in the figure legends. Population genotype distribution was analyzed by χ^2 test. Two-way ANOVA was used when comparing two variables (genotypes and drugs). Bonferroni's test, Dunnet's test, and t test were used for *post hoc* comparisons depending on the experiments. One-way ANOVA test was used for multiple group com-

parisons followed by Tukey's or Bonferroni's *post hoc* test. Student's unpaired two-tailed t test was used when two groups were compared. $p < 0.05$ was predetermined as the threshold for statistical significance.

Results
Generation of DAT-KO rats
Slc6a3 (DAT) KO rats were generated by SAGE Laboratories. DAT-KO rats were created by using ZFN technology that produces a 5 bp mutation and an early stop codon (Fig. 1A). The targeted DNA to be deleted (*Slc6a3* exon 2) contained a specific nucleotide sequence substrate for restriction enzyme BtsIMutI. According to our genetically modified model, disruption of this specific sequence causes the loss of restriction site for BtsIMutI enzyme, resulting in WT rats maintaining all restriction sites on both alleles, whereas DAT-HET rats bear one truncated allele and an intact one. DAT-KO rats lose both restriction enzyme sites as predicted (Fig. 1B). PCR primers were designed according to protocol and amplified DNA was digested as shown (Fig. 1B,C). In DAT-KO rats, no detection of digestion product was observed due to the loss of restriction site on both alleles. DAT-HET rats show both the digested DNA at lower molecular weight and mutated DNA, whereas WT DNA amplicon was completely digested by BtsIMutI, thus resulting in

one single band at lower molecular weight (Fig. 1 B,C). We also verified the absence of DAT protein in KO animals in Western blot from striatal tissue (Fig. 1D and Fig. 1-1, available at https://doi.org/10.1523/JNEUROSCI.1931-17.2018.f1-1).

Although there are reasonable concerns for potential off-targeting effects of gene editing nucleases (including ZFN) technologies, there are little chances for these events in DAT-KO rats. First, the ZFN designs were generated using a proprietary algorithm by bioinformatics team at SAGE Laboratories that screens each design for the top 20 most homologous sequences, as well as for repeat elements, SNPs, and splice variants. In addition, the ZFN used in this study contains specifically engineered obligate heterodimer FokI cleavage domains that help to guard against off-targeting by increasing specificity to cut at only the desired site. In any case, founder animals were bred back to WT Wistar Han rats (Charles River Laboratories) for six generations. This should be sufficient to minimize the chances of any potential unintended off-target effects that may have occurred even with rigorous screening in the ZFN design and construction phase. Assuming hypothetical, unlinked off-target modifications will be diluted through breeding, an indirect way to detect potential off-target events could be to compare phenotypically early-generation with later-generation homozygotes. The lack of difference in phenotypes implies the absence of off-target events. Animals starting from the third generation of backcrossing were used in neurochemical and locomotor activity studies. For all other experiments, we used animals after the sixth generation of backcrossing. No difference in the locomotor hyperactivity of early-generation and later-generation homozygotes was observed. The Wistar Han DAT-KO rat colony was kept under HET–HET breeding. Surprisingly, DAT-KO rats do not show a propensity to premature death as DAT-KO mice (Giros et al., 1996), although it might depend on the genetic background because, for example, in F1 D2/B6 hybrid mice no such lethality was present (Morice et al., 2004). They are viable as the WT controls and population genotype distribution at age 4 months was not significantly different ($\chi^2 = 1.7$; DF = 2; $p = 0.4275$, χ^2 test) from expected Mendelian distribution 1:2:1, resulting from HET–HET mating (Fig. 1E). Analysis of body weight from birth up to adulthood (4 months) revealed a major effect of genotype in both male (Fig. 1F; 2-way ANOVA; F interaction = 58,40; $p = 0.0001$) and female (Fig. 1F; 2-way ANOVA; F interaction = 11,11; $p = 0.0001$) populations, with DAT-KO animals showing lower weights compared with HET and WT siblings. At the same time, no difference in food intake was found between genotypes (Fig. 1G).

Neurochemical characterization of striatal DA transmission in DAT-KO rats
Analysis of DA dynamics by FSCV
To evaluate the consequences of DAT gene deletion on the extracellular dynamics of DA, we used the FSCV technique on brain slices (Jones et al., 1998). First, we detected the kinetics of evoked DA release and clearance after single-pulse (400 μA, 1 ms, biphasic) stimulation in striatal slices prepared from DAT-KO, DAT-HET, and WT littermates. The oxidation peak occurred at $\sim +0.6$ V and the reduction peak at ~ -0.2 V (Fig. 2A, insert), consistent with the electrochemical characteristics of DA (Jones et al., 2006; John and Jones, 2007; Bradaia et al., 2009; Leo et al., 2014). The maximal amplitude of DA overflow evoked by single pulses in the DStr was not significantly different between genotypes, but the clearance of released DA was markedly prolonged in DAT-HET and DAT-KO rats (Fig. 2A–C). We evaluated the uptake kinetics from an exponential fit curve using a least-squares-

constrained exponential fit algorithm (Yorgason et al., 2011) and quantified the half-life parameters for an estimation of DA uptake rates. Under basal conditions, the time to clear released DA was 1.3, 10, and 50 s, respectively, in WT, DAT-HET, and DAT-KO rats (Fig. 2B).

Next, we evaluated the effect of COC on evoked DA release and clearance. As it might be expected, application of 3 μM COC progressively prolonged an amplitude of striatal DA outflow and clearance (John and Jones, 2007) in WT and DAT-HET, but not in DAT-KO rats (Fig. 2C,D). Further, to test whether the serotonin transporter (SERT) could provide extracellular DA clearance via promiscuous uptake, we applied 10 μM fluoxetine, a selective SERT blocker. As shown in Figure 2E, fluoxetine did not affect DA clearance in any of the genotypes. To evaluate whether DA-metabolizing enzymes can contribute to the clearance of DA in the absence of DAT, we then tested the effect of the inhibition of catechol-O-methyl-transferase (COMT) by 10 μM tolcapone (Fig. 2F) and monoamine oxidase (MAO) by 10 μM pargyline (Fig. 2G). COMT inhibition did not alter the kinetics of DA clearance in any genotype, whereas inhibition of MAO did not affect released DA half-life in WT or DAT-HET animals but prolonged it in DAT-KO rats (Fig. 2 F,G).

Analysis of extracellular DA levels by in vivo *microdialysis*
To evaluate the consequences of disrupted DA clearance on the basal extracellular DA levels, we applied a quantitative low perfusion rate microdialysis approach to freely moving animals, which, unlike conventional microdialysis, provides a true measure of extracellular neurotransmitter concentrations (Bradaia et al., 2009; Leo et al., 2014). As expected, DAT-KO and DAT-HET rats showed an increased amount of basal extracellular DA levels in the striatum, with an $\sim$8-fold and 3-fold increase over WT levels, respectively (Fig. 3A). Levels of the DA metabolites DOPAC and HVA were elevated in DAT-KO rats only. Furthermore, to assess the effects of AMPH on striatal DA release, we administered AMPH and monitored the extracellular levels of DA in the striatum of freely moving rats by a conventional microdialysis. As expected, AMPH produced a genotype-dependent effect (Fig. 3D–F). AMPH induced a significant increase in extracellular DA in WT and to a lesser degree in DAT-HET rats. At the same time, no effect was found in animals lacking DAT.

Striatal tissue DA, 5-HT and metabolites
We next evaluated the total tissue content of monoamines and their metabolites in the striatum (Fig. 3G). As in DAT-KO mice (Jones et al., 1998), we observed a pronounced reduction in total tissue DA levels in DAT-KO rats ($\sim$13-fold; Fig. 3G) compared with control and HET animals. At the same time, the levels of an intraneuronal DA metabolite DOPAC and predominantly extracellular DA metabolite HVA, appeared to be significantly increased in DAT-KO rats. Similar to DAT-KO mice (Jones et al., 1998), striatal 5-HT levels were decreased in DAT-KO rats, with no changes observed in 5-HIAA levels.

Expression profile of selected DA-related genes in striatal samples
To evaluate the consequences of remarkable changes in the extracellular DA due to absence of reuptake process, we evaluated by real-time PCR the expression of genes critical for DA homeostasis in the midbrain and striatum as well as TH protein levels in the striatum by Western blot. In the midbrain of DAT-KO rats, TH mRNA was decreased (Fig. 3H), with even more pronounced decrease of TH protein levels in the striatum (Fig. 3I). A similar decrease was reported previously in DAT-KO mice (Jaber et al., 1999). DAT-KO rats, similarly to mice (Giros et al., 1996), also
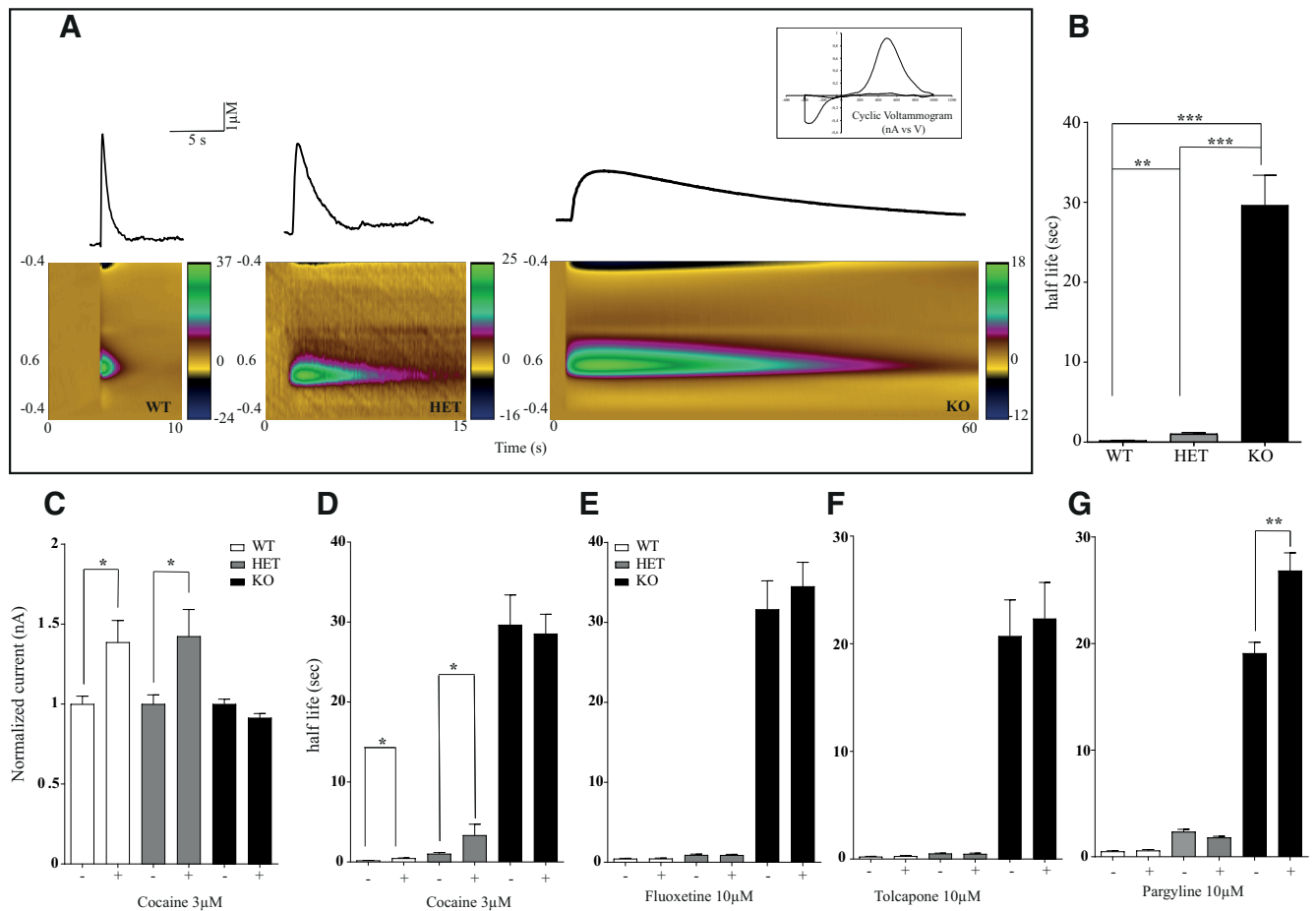
Figure 2. Recording of electrically stimulated DA efflux in striatal brain slices from DAT-KO rats. **A**, A single biphasic stimulus (400 μA, 1 ms) was used to evoke DA release in striatal brain slices from WT, DAT-HET, and DAT-KO rats. The average time to clear released DA was 1.3, 10, and 50 s respectively. Bottom, Color plot representing the voltammetric currents (encoded in color in the z-axis) plotted against the applied potential (y-axis) and time (x-axis). Top, Cyclic voltammogram identifying the detected analyte as DA. **B**, Kinetics of evoked DA release in DStr of DAT WT, DAT-HET, and DAT-KO. **C, D**, Effect of 3 μM COC on evoked DA release. COC had no effect on evoked DA overflow in DAT-KO rat but induced the well known increase in DA overflow in both WT and DAT-HET (**C**) COC-induced changes in extracellular DA half-life (**D**). **E**, Fluoxetine (10 μM) effect on evoked DA release. **F**, Tolcapone (10 μM) effect on DA release. **G**, Pargyline (10 μM) effect on evoked DA release ($n = 5–6$ per each group, *$p < 0.05$; **$p < 0.01$; ***$p < 0.001$).

showed decreased levels of both the dopamine D1 receptor (D1R) and the dopamine D2 receptor (D2R) in the striatum in response to persistently elevated extracellular DA (Fig. 3J,K, respectively).

Behavioral phenotyping of DAT-KO rats

Locomotor activity tests
It is well known that alterations in DAT function cause pronounced changes in locomotor behavior by influencing the dopaminergic tone in the basal ganglia (Giros et al., 1996). We evaluated the locomotor activity of mutant rats in home cages during 24 h and observed a significantly altered pattern of motor activity in DAT-KO animals that varied according to the light/dark cycle, increasing significantly during the night compared with WT and HET siblings (Fig. 4A). Locomotor activity of DAT rats was also assessed in a novel environment under illuminated conditions using activity chambers. Total distance traveled and vertical locomotor activity counts were recorded in 1.5-, 2.0-, 2.5-, 3.0-, and 4.0-month-old animals (Fig. 4B,C). In each tested age, total distance traveled by DAT-KO rats was highly elevated comparing WT and DAT-HET animals, with a characteristic of DAT-KO mice of perseverative locomotor pattern of activity (Ralph et al., 2001). DAT-KO rats also displayed prominent vertical activity at all tested ages (Fig. 4D,E).

Next, we evaluated the effects of compounds that are known to suppress hyperactivity of DAT-KO mice (Gainetdinov, 2008). Among them, the most noticeable are the psychostimulants AMPH and MPH used in the treatment of ADHD (Gainetdinov et al., 1999). Administration of AMPH (1, 2, 3, and 4 mg/kg, i.p.) to DAT-KO animals had a paradoxical calming effect in hyperactive DAT-KO animals, with the most significant effect starting from 2 mg/kg AMPH (Fig. 4F,H). In WT and HET rats, treatment with this psychostimulant produced a significant increase in locomotor activity (Fig. 4F,H). Similar results were obtained with MPH (Ritalin), the drug of choice in the treatment of ADHD. Administration of 1.5, 2.5, and 5 mg/kg MPH dose dependently reduced hyperlocomotion in DAT-KO animals (Fig. 4F,H) while inducing a strong increase in WT and DAT-HET rats. Recent studies have revealed that Trace Amine-Associated Receptor 1 (TAAR1) can regulate the DA system and affect dopamine-related behaviors. As it has been shown previously in DAT-KO mice (Revel et al., 2011), the partial TAAR1 agonist RO5203648 effectively reduced the hyperlocomotor behavior of DAT-KO rats without a significant effect in control and DAT-HET animals (Fig. 4F,H). We finally demonstrated that the administration of the typical antipsychotic drug, haloperidol (0.5

mg/kg, s.c.), potently reversed hyperloco-motion in DAT mutant rat model, as it does in DAT-KO mice (Gainetdinov et al., 1999). Haloperidol administration also reduced the locomotor activity of WT and DAT-HET rats (Fig. 4G,I).

Cognitive tests and schedule-induced polydipsia

To evaluate the consequences of DAT-deficiency-related hyperdopaminergia on the cognitive abilities of rats, we first used the Y-maze task. The performance of the rats in the Y-maze task is expressed as a percentage and refers to ratio of arm choices differing from the previous two choices to the total number of arm entries. DAT-KO rats alternated between the arms of the maze significantly less than WT and HET rats ($F_{(2,24)} = 11.944$, $p = 0.0003$), indicating deficiency in working memory (Fig. 5A). Importantly, analysis of food consumption (*ad libitum*) revealed no difference in food intake between genotypes (Fig. 1G).

Schedule-induced polydipsia is excessive drinking induced by a particular sub-optimal schedule of food reinforcement that is considered to model compulsive behaviors in rats (Alonso et al., 2015). The polydipsia induced by the FT 60 s schedule of reinforcement was successfully established in WT (15.9 ± 1.7 ml) and DAT-HET (10.4 ± 1.3 ml) rats, but not in DAT-KO rats (2.5 ± 0.7 ml) (Fig. 5B). After the rank transformation, data were subjected to one-way ANOVA, which demonstrated a significant effect of genotype ($F_{(2,42)} = 23,078$, $p = 0.00001$). *Post hoc* analysis (Bonferroni's test) revealed that WT rats consumed more water than DAT-HET rats and both WT and DAT-HET rats consumed more than DAT-KO rats.

Finally, DAT-KO rats showed a significant difference also in the startle response and prepulse inhibition test, which are used to assess sensorimotor gating functioning (Fig. 5C,D). DAT-KO rats showed an increased startle response amplitude and impaired prepulse inhibition compared with WT and DAT-HET rats. Two-way ANOVAs revealed significant differences

←

increased metabolites DOPAC and HVA levels (n = 5–6). **H–J**, Molecular profile of selected DA-related genes in striatal samples. **H**, TH mRNA expression is decreased in DAT-KO midbrain samples. **I**, TH protein levels in the striatum are decreased in DAT-KO rats. **J**, D1R mRNA levels are decreased in both DAT-HET and DAT-KO striatal samples. **K**, D2R mRNA levels are reduced in DAT-KO striatal samples. (n = 6; one-way ANOVA; *p < 0.05; **p < 0.01; ***p < 0.001).
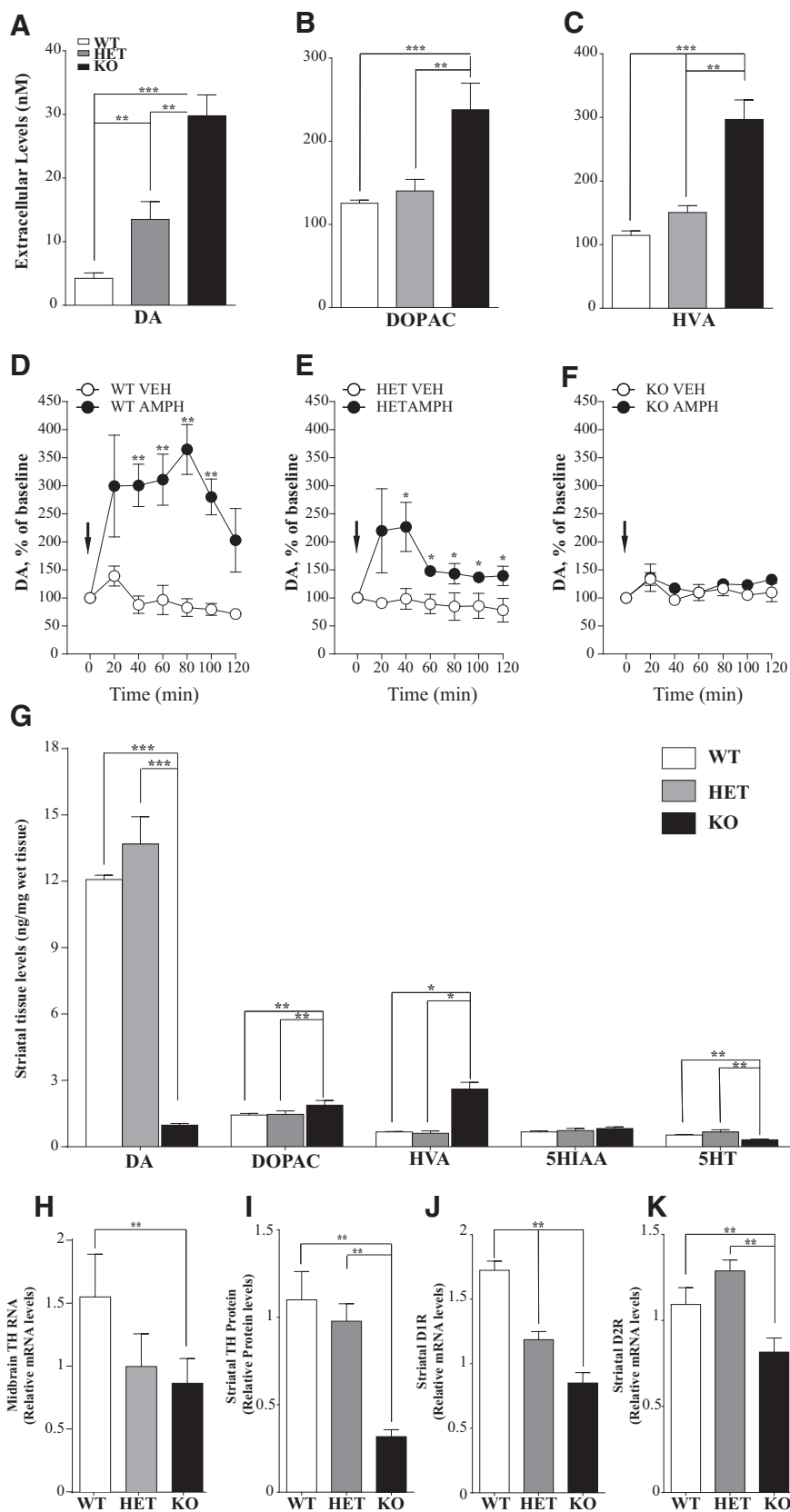
Figure 3. Neurochemical profile of striatal DA transmission in DAT-KO rats. **A–C**, Quantitative low perfusion rate microdialysis in freely moving rats showed an increased amount of extracellular DA (**A**) and both DA metabolites, DOPAC (**B**), and HVA (**C**) in the striatum of DAT-KO rats. Results are the mean ± SEM of six independent experiments. **D**, **E**, **F**, Effect of AMPH (2 mg/kg, i.p.) on extracellular DA levels measured by conventional microdialysis in the striatum of freely moving rats. Results are the mean ± SEM of six independent experiments. **G**, HPLC analysis on striatal samples showed a 13-fold decrease in total tissue DA levels, along with

both in startle response ($F_{(2,42)} = 7.35$, $p = 0.01$) and prepulse inhibition ($F_{(2,42)} = 21.11$, $p = 0.001$) (for significance level of single points, see Fig. 5C,D). No differences were found between WT and DAT-HET rats (all $p > 0.05$).

Analysis of BDNF transmission in DAT-KO rats

In an attempt to investigate the putative mechanisms responsible for the cognitive impairment in DAT-KO rats, we evaluated the pattern of BDNF expression and related signaling in the rat PFC (Fig. 5E–H). Figure 5E shows that, total BDNF mRNA levels are reduced in the PFC of DAT-KO rats (-12%, $t_{(8)} = 3.2$; $p = 0.013$). To get further insights into the complex organization of the BDNF gene, we investigated the modulation of several transcripts for which expression is driven by separate promoters (Aid et al., 2007). We focused our analysis on BDNF exon IV, the most abundant transcript whose transcription that is activity dependent, and exon VI, primarily targeted to dendrites (Pruunsild et al., 2011). Interestingly, the analysis of these different BDNF transcripts revealed that such decrease could be ascribed to BDNF exon IV (-20%, $t_{(8)} = 4.43$; $p = 0.002$) because no changes were seen in BDNF exon VI ($+2\%$, $t_{(8)} = 0.26$; $p = 0.80$; Fig. 5E). We thus restricted our analysis to the regulation of the promoter responsible for the transcription of BDNF exon IV by investigating its main transcription factors. We found reduced gene expression of CaRF (-21%, $t_{(8)} = 4.15$; $p = 0.003$) and neuronal Per-Arnt-Sim domain protein 4 (Npas4) (-40%, $t_{(8)} = 5.41$; $p = 0.0006$), with no changes in Creb (Fig. 5F). Because the reduction of CaRF mRNA levels may suggest defective processes mediating calcium influx, we measured the activity of Ca^{2+}/calmodulin-dependent protein kinase II (αCaMKII), which is known to be acti-

←

were evaluated for 4 h. The results are expressed as the mean ± SEM. * and #$p < 0.001$ (Bonferroni's test) relative to the corresponding WT or DAT-HET groups ($n = 6-20$ per group). **F–I**, Drug effects on vertical activity and total distance traveled of DAT-KO rats. Before drug administration, the rats were habituated to the activity monitor for 30 min. After drug injection, the locomotor activity of the animals was recorded for additional 70 min or 90 min (haloperidol). Total distance covered (**F, G**) and the vertical activity (**H, I**) counts for 60 min (from 40–100 min) for all drugs (**F, H**) or 90 min (from 30–120 min) for haloperidol (**G, I**) were used for subsequent analysis. The results are expressed as the mean ± SEM. *$p < 0.05$ (Dunnett's test, t test), relative to the corresponding saline-treated control groups. $n = 6-19$ per group, with exception of DAT-HET rats treated with haloperidol, for which $n = 4$.
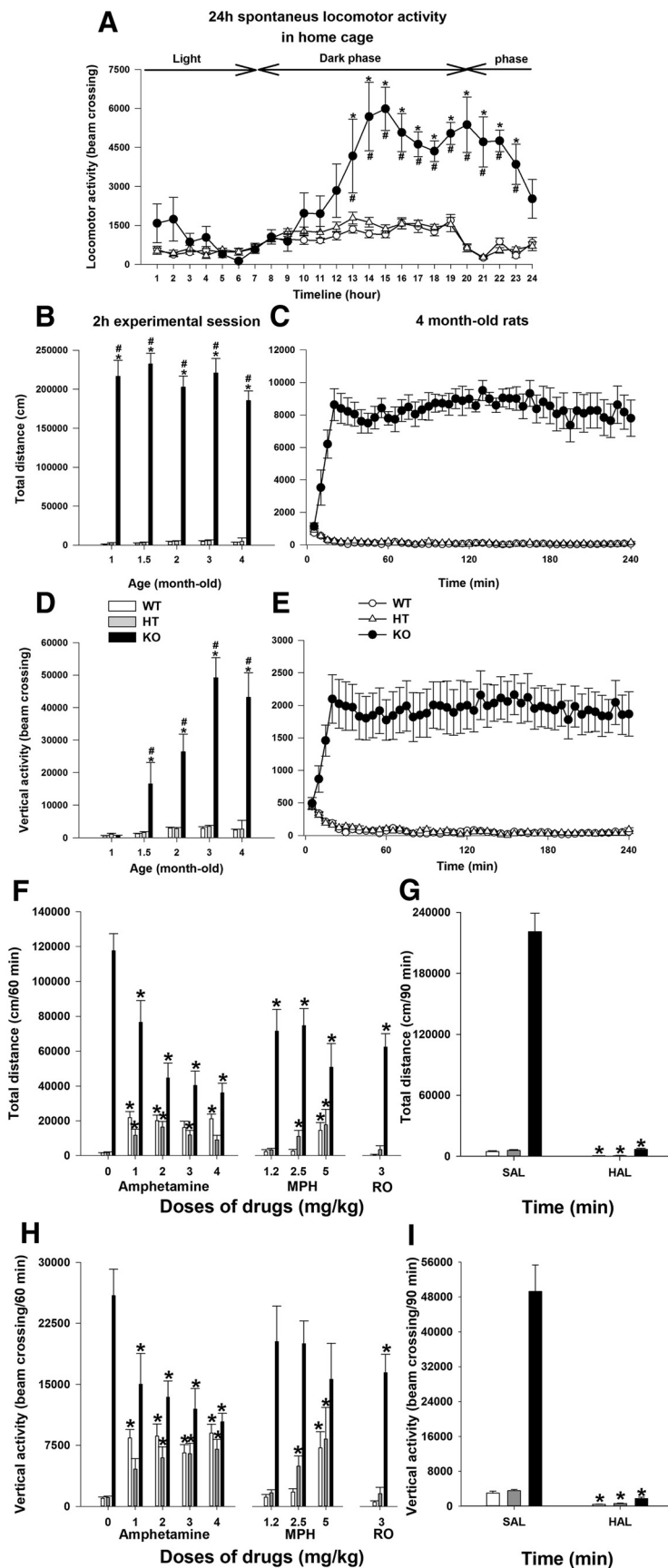
Figure 4. Basal and drug-modified locomotor activity of DAT-KO rats. **A**, Locomotor activity of adult animals was recorded in home cages for 24 h. **B, D**, Total distance traveled and vertical activity of animals in different ages were assessed using an automated Omnitech Digiscan locomotor activity chambers for 2 h. **C, E**, Total distance and vertical activity of 4-month-old animals
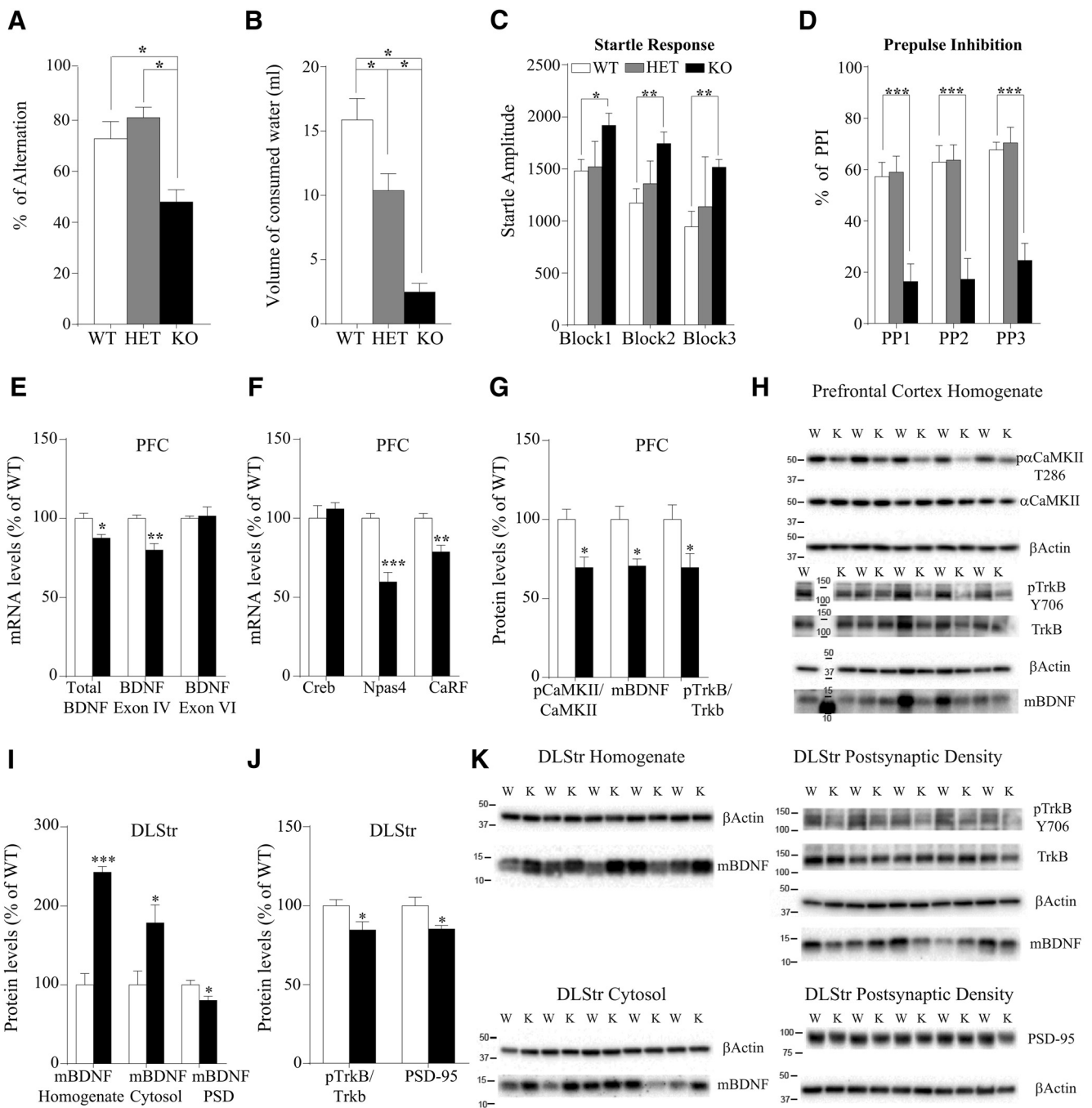
Figure 5. Cognitive dysfunction and altered BDNF transmission in DAT-KO rats. *A*, Spontaneous alternation test. To measure spontaneous alternation behavior and exploratory activity, a white plastic material Y-maze with arms 40 cm (long) by 6 cm (wide) with 13 cm walls was used. Each animal was tested in a single 8 min session during which the animal was placed in the central platform and allowed free exploration of the maze. Spontaneous alternation, expressed as a percentage, refers to ratio of arm choices differing from the previous two choices to the total number of arm entries. The percentage of alternation observed is strongly reduced in DAT-KO animals. Values are expressed as mean ± SEM of $n = 8$ rats/group. One-way ANOVA followed by Bonferroni's test. *$p < 0.05$, with respect to WT and DAT-HET rats. *B*, Schedule-induced polydipsia induced by fixed-time 60 s schedule of reinforcement. The polydipsia induced by FT 60 s schedule of reinforcement was successfully established in WT and DAT-HET, but not in DAT-KO rats. After the rank transformation, data were subjected to one-way ANOVA, which demonstrated a significant effect of genotype. *Post hoc* analyses (Bonferroni's test) revealed that WT rats consumed more water than DAT-HET and DAT-KO rats, whereas DAT-HET rats consumed more than DAT-KO rats ($p < 0.05$). Values are expressed as mean ± SEM ($n = 9$–18). *C*, *D*, Startle response (*C*) and PPI of the startle response (*D*). The day of the test, rats were transferred into the experimental room under environmentally controlled conditions (sound proof and red dim lights) and, after 30 min of habituation, were positioned in the apparatus and startle response and prepulse inhibition assessed (see Materials and Methods). Values are expressed as mean ± SEM of $n = 8$ rats/group. Block1, Block2, and Block3 indicate the three consecutive sequences of stimuli of the test. PP1, PP2, and PP3 indicate the three different intensities of the prepulse stimulus. Two-way ANOVA followed by Bonferroni's test. *$p < 0.05$, **$p < 0.01$, ***$p < 0.001$ with respect to WT rats. *E*, Total BDNF and BDNF exon IV mRNA levels are reduced in the PFC of DAT-KO rats, whereas no changes were observed in the mRNA levels of BDNF exon VI. *F*, Analysis of the transcription factors involved in the modulation of BDNF exon IV revealed a significant reduction in the expression of Npas4 and CaRF and no changes in Creb mRNA levels. *G*, *H*, Activation of αCaMKII is reduced in the PFC homogenate of DAT-KO rats. The transcriptional changes of BDNF were paralleled by a reduction in the mBDNF levels and accompanied by reduced activation of trkB in the PFC homogenate of DAT-KO rats. *H*, Original immunoblots used to generate data presented in *G*. W-WT, K-KO rats. *I*, *K*, In the DLStr, mBDNF levels are increased in the homogenate and in the cytosol but reduced in the postsynaptic density. *J*, *K*, trkB activation and PSD-95 levels are reduced in the postsynaptic density of DLStr of DAT-KO rats. Data are presented as percentage of WT levels. *K*, Original immunoblots used to generate data presented in *I* and *J*. W, WT; K, KO.

vated by calcium. As shown in Figure 5, G and H, the activation of αCaMKII (as reflected by the ratio between the phosphorylated and the respective total form) is significantly reduced in the PFC of DAT KO rats (-30%, $t_{(8)} = 3.30$; $p = 0.011$). We then measured mBDNF protein levels in the PFC and found it reduced (-30%, $t_{(8)} = 3.12$; $p = 0.014$). Similarly, we found a significant reduction in the activation of the high-affinity BDNF receptor trkB (-30%, $t_{(8)} = 2.38$; $p = 0.044$; Fig. 5G,H).

We then measured mBDNF expression and signaling in the DLStr. Figure 5, I and K, shows that lack of DAT induces the subcellular redistribution of the neurotrophin in this brain region because mBDNF is increased in the cytosol of DLStr but reduced in the postsynaptic density (homogenate: $+143\%$, $t_{(7)} = 9.56$; $p < 0.0001$; cytosol: $+78\%$, $t_{(7)} = 2.59$; $p = 0.036$; postsynaptic density: -20%, $t_{(8)} = 2.53$; $p = 0.035$). Additionally, in the postsynaptic density of the DLStr, we found reduced expression and phosphorylation of the high affinity BDNF receptor, trkB (-15%, $t_{(8)} = 2.38$; $p = 0.045$; Fig. 5J,K) suggesting a reduced BDNF-mediated signaling in DAT-KO rats. As the interaction between dopaminergic and glutamatergic systems in the striatum are important for cognitive processing, we examined the expression of a critical determinant of glutamate transmission, PSD-95, as an index of glutamate spine density, and found a reduced expression of PSD-95 in the striatum of DAT-KO rats compared with WT counterparts (-21%, $t_{(8)}$ 2.57; $p = 0.033$; Fig. 5J,K).

Discussion

The involvement of DA neurotransmission in several physiological and pathological conditions has led to intense studies on animal models of dopaminergic dysfunction. One such model, DAT-KO mice, has provided numerous advances in understanding the role of DA in these disorders (Giros et al., 1996; Gainetdinov, 2008). Here, we describe the rat KO model of DAT deficiency that provides certain advantages compared with the mouse model. Rat models offer many powerful advantages: the larger size means larger tissues and samples that can lead to a reduction in the number of animals required for a study. Moreover, the larger size of the rat allows surgeries that are much easier to perform, particularly in small brain areas. Rats are particularly far superior to mice when it comes to behavioral assays: they perform much more reliably and robustly than mice and mouse behavioral assays typically require larger cohort sizes than those needed for rats due to increased variability.

Viability of DAT-KO rats
DAT-KO rats are viable and demonstrate the expected Mendelian ratio from birth up to 4 months of age. By comparison, DAT-KO mice showed a continuous decrease in survival rate starting from 4 weeks of age, with ~35% of mutants demonstrating neurological dysfunctions and death due to postsynaptic neurodegeneration (Cyr et al., 2003), although this may depend on genetic background of mice (Morice et al., 2004). Like mutant mice (Bossé et al., 1997), DAT-KO rats develop normally but weigh less than HET and WT control animals, an effect independent of food intake.

Dysregulation of striatal DA transmission in DAT-KO rats
To evaluate the neurochemical consequences of the absence of DAT on striatal DA transmission, we first measured real-time extracellular DA dynamics after evoked release using FSCV. As in DAT-KO mice (Jones et al., 1998), DA persists for a protracted period in the synaptic cleft in DAT-HET and DAT-KO rats. The clearance of extracellular DA was ~40-fold slower in the striatum of DAT-KO compared with WT controls, whereas it was de-

creased approximately twofold in DAT-HET rats. The extracellular half-life of evoked DA in the striatal slices of DAT-KO animals was not altered by COC, fluoxetine, or the COMT inhibitor tolcapone. It was somewhat prolonged by MAO inhibitor pargyline, indicating that, whereas diffusion is the major mechanism available to eliminate DA from the extracellular space in the absence of DAT (Jones et al., 1998), there is some minor contribution of MAO in DA clearance as well (Benoit-Marand et al., 2000). As in DAT-KO mice (Jones et al., 1998), prolonged extracellular lifetime of released DA resulted in an approximately threefold and sevenfold increase in striatal basal extracellular levels of DA in DAT-HET and DAT-KO rats, respectively. At the same time, as in DAT-KO mice, total tissue content of striatal DA was reduced 13-fold, indicating the critical contribution of DAT-mediated transport of DA in maintenance of intraneuronal stores of DA (Jones et al., 1998). The only neurochemical difference detected was a significant increase in total tissue concentration of DOPAC, presumably indicating a more prominent role of MAO in metabolism of DA in rats compared with mice. As for COC in FSCV experiments, AMPH effects on striatal extracellular DA levels were absent in DAT-KO and reduced in DAT-HET rats, indicating the critical role of DAT in the effects of this psychostimulant. The absence of DAT and the persistent elevation of DA in the synaptic cleft produced profound variation in key DA-related genes. As in DAT-KO mice (Giros et al., 1996), striatal mRNA levels of the two major DA receptors, D1R and D2R, were significantly decreased. At the same time, midbrain mRNA and striatal protein levels of the rate-limiting enzyme for DA biosynthesis, TH, were decreased in DAT-KO rats, supporting previous observations in DAT-KO mice (Jaber et al., 1999).

Hyperactivity of DAT-KO rats
The most prominent phenotype of DAT-KO rats is the hyperlocomotion determined by an increased DA tone in basal ganglia. DAT-KO rats showed an intense locomotor activity both in a new environment and in the home cages. The hyperlocomotion of homozygous KO rats persists during the lifespan and, as already seen in DAT-KO mice, is greater than the effect produced by DAT blocker drugs (Giros et al., 1996). As in DAT-KO mice, AMPH and MPH significantly reduced locomotor activity of DAT-KO rats while inducing the well known increase in DAT-HET and WT animals (Gainetdinov et al., 1999). The psychostimulatory actions of AMPH and MPH are primarily dependent on a direct interaction of these compounds with DAT, leading to elevated DA (Fumagalli et al., 1998; Chen et al., 2006; Thomsen et al., 2009). Because DAT-KO rats lack the major target of AMPH action, the "calming" effect of psychostimulants suggests the involvement of a DAT-independent mechanism of action, possibly involving other monoamine transporters. Interestingly, we observed an inhibitory action of MPH at lower (~10-fold) doses in rats compared with mice (Gainetdinov et al., 1999), suggesting significant differences in pharmacodynamic or pharmacokinetic properties of this drug between these species. Hyperactivity and paradoxical inhibitory effects of psychostimulants used in the treatment of ADHD could be a first indication of face and predictive validity of DAT-KO rats as an improved animal model for this disorder. Moreover, the ability of the partial TAAR1 agonist RO5203648 to modulate the locomotor behavior of DAT-KO rats supports the potential of TAAR1 as a target for therapeutic intervention in DA-related disorders. Previous data showed that activation of TAAR1 strongly regulates DA transmission and reduces DA-dependent behavioral effects of psychostimulants as well as hyperactivity of DAT-KO mice (Bradaia et al., 2009; Revel

et al., 2011; Leo et al., 2014) likely via an interaction of TAAR1 with D$_2$R or with different neurotransmitter pathways such as the glutamatergic pathway (Espinoza et al., 2015).

DAT-KO rats show DA-related cognitive deficits and tolerance to the development of compulsive behavior

As an indication of DA-related cognitive deficits, DAT-KO rats, like DAT-KO mice, show an impaired sensorimotor gating measured as reduced PPI of the acoustic startle reflex (Ralph et al., 2001). DA hyperactivation, induced by pharmacological interventions or genetic manipulation of DAT, causes PPI deficits in experimental animals similar to those observed in psychiatric disorders such as schizophrenia and ADHD (Braff et al., 2001; Swerdlow et al., 2001; Yamashita et al., 2006; Arime et al., 2012). DAT-KO rats show also a decreased Y-maze spontaneous alternation that indicate an impaired working memory function. Because intact dopaminergic signaling in the PFC seems to be required for correct mnemonic function (Goldman-Rakic, 1996; Kesner and Rogers, 2004), we can postulate that absence of DA reuptake could impair the retention of short-term memory information in DAT-KO rats. At least some of these dopaminergic effects may involve D1Rs (Lidow et al., 1991; Goldman-Rakic et al., 1992; Gaspar et al., 1995).

Schedule-induced polydipsia (SIP) is an adjunctive model in which animals exhibit exaggerated drinking (polydipsia) when presented with food pellets under a fixed-time schedule. SIP is one of the best established tests of compulsive behaviors in rats that is commonly used to model obsessive-compulsive disorder (OCD) (Alonso et al., 2015). Dopaminergic neurotransmission plays an important role in the development and maintenance of SIP (for review, see Moreno and Flores, 2012). The lack of SIP development in DAT-KO animals is consistent with several reports showing that AMPH is able to attenuate SIP dose dependently (Sanger, 1977; Flores and Pellón, 1997). Interestingly, that ADHD and OCD are often considered as disease antipodes with the significant difference in brain biochemistry (Carlsson, 2000). Thus, our results, indicating a deficit in the development of compulsive behavior in DAT-KO rats might further support the use of these mutant animals as a valuable model related to ADHD.

Frontostriatal BDNF dysregulation in DAT-KO rats

In an attempt to find a molecular correlate of the above shown cognitive deficit, we focused our attention on the neurotrophin BDNF, which plays a role in working memory (Egan et al., 2003) and the expression of which was found to be developmentally dysregulated in the PFC of DAT-KO mice (Fumagalli et al., 2003). We found that DAT deletion in rats reduces total BDNF mRNA levels in the PFC. Further, analysis of the main different transcripts produced by the activation of the different promoters at 5′-UTR revealed that only BDNF exon IV is reduced. Because this transcript is tightly dependent on neuronal activity, we suggested that activity-dependent gene expression is impaired in these rats. Moreover, the analysis of the transcription factors involved in the modulation of BDNF exon IV showed that the expression of the neuronal transcription factor NPAS 4, an immediate early gene selectively induced by neuronal activity (Sun and Lin, 2016), is reduced as well. The expression of CaRF, which also regulates BDNF exon IV expression, is reduced, suggesting reduced calcium influx; this was corroborated by the reduced activation of αCaMKII, a well known intracellular calcium sensor required for CaRF activity (Zheng et al., 2011). Given that both calcium influx and αCaMKII activation often represent the first stimulus for activity-dependent gene expression in neurons

(Fields et al., 2005), we suggested defective calcium influx as a potential mechanism for the impairment in the cortical-activity-dependent gene expression in the PFC of DAT KO rats. Changes in BDNF mRNA levels were accompanied by a downregulation of BDNF protein levels, suggesting that DAT deletion regulates also the translation of the neurotrophin. We also found reduced activation of the high-affinity BDNF receptor trkB, suggesting that, in the PFC of DAT KO rats, BDNF-mediated transmission is impaired, an effect that may contribute to the impaired working memory function (Galloway et al., 2008).

Our analyses revealed that the removal of DAT also altered the BDNF system in the DLStr, where it results in a redistribution of the neurotrophin. In the whole homogenate, we found increased expression of BDNF leading to the activation of trkB and its downstream intracellular signaling; however, the removal of DAT leads to increased BDNF expression in the cytosol while reducing its expression, together with its downstream signaling, in postsynaptic density. This observation may have a relevant and functional effect, given the well established role of BDNF in the control of glutamatergic spine density (Young et al., 2015) and since reduced spine density was reported in striatal medium spiny neurons of DAT-KO mice (Berlanga et al., 2011). In fact, in line with the herein shown reduced BDNF expression, we also found a decreased expression of the marker of glutamatergic spines PSD-95, as previously observed in DAT-KO mice (Yao et al., 2004), suggesting potential structural rearrangements of glutamate synapses in the DLStr.

Conclusions

Together, these observations indicate that DAT-KO rats represent an improved model of persistently increased dopaminergic transmission that is presumably involved, at least in part, in endophenotypes of such disorders as schizophrenia, bipolar disorder, ADHD, and Huntington's disease (Carlsson, 1987; Howes and Kapur, 2009; Gardoni and Bellone, 2015; Bonvicini et al., 2016; Vengeliene et al., 2017). These rats have obvious advantages over mouse models by showing increased survival rate, larger brain size allowing investigations of smaller brain regions, and being closer physiologically to humans. Because the behavioral repertoire of rats is significantly more complex compared with mice, mutant rats could be particularly useful to evaluate the effects of novel therapeutics on cognitive functions.

References

Aid T, Kazantseva A, Piirsoo M, Palm K, Timmusk T (2007) Mouse and ratBDNF gene structure and expression revisited. J Neurosci Res 85:525–535. CrossRef Medline

Alonso P, López-Solà C, Real E, Segalàs C, Menchón JM (2015) Animal models of obsessive-compulsive disorder: utility and limitations. Neuropsychiatr Dis Treat 11:1939–1955. CrossRef Medline

Arime Y, Kasahara Y, Hall FS, Uhl GR, Sora I (2012) Cortico-subcortical neuromodulation involved in the amelioration of prepulse inhibition deficits in dopamine transporter knockout mice. Neuropsychopharmacology 37:2522–2530. CrossRef Medline

Beaulieu JM, Sotnikova TD, Marion S, Lefkowitz RJ, Gainetdinov RR, Caron MG (2005) An Akt/beta-arrestin 2/PP2A signaling complex mediates dopaminergic neurotransmission and behavior. Cell 122:261–273. CrossRef Medline

Benoit-Marand M, Jaber M, Gonon F (2000) Release and elimination of dopamine in vivo in mice lacking the dopamine transporter: functional consequences. Eur J Neurosci 12:2985–2992. CrossRef Medline

Berlanga ML, Price DL, Phung BS, Giuly R, Terada M, Yamada N, Cyr M, Caron MG, Laakso A, Martone ME, Ellisman MH (2011) Multiscale imaging characterization of dopamine transporter knockout mice reveals regional alterations in spine density of medium spiny neurons. Brain Res 1390:41–49. CrossRef Medline

Bonvicini C, Faraone SV, Scassellati C (2016) Attention-deficit hyperactiv-

ity disorder in adults: a systematic review and meta-analysis of genetic, pharmacogenetic and biochemical studies. Mol Psychiatry 21:872–884. CrossRef Medline

Bossé R, Fumagalli F, Jaber M, Giros B, Gainetdinov RR, Wetsel WC, Missale C, Caron MG (1997) Anterior pituitary hypoplasia and dwarfism in mice lacking the dopamine transporter. Neuron 19:127–138. CrossRef Medline

Bradaia A, Trube G, Stalder H, Norcross RD, Ozmen L, Wettstein JG, Pinard A, Buchy D, Gassmann M, Hoener MC, Bettler B (2009) The selective antagonist EPPTB reveals TAAR1-mediated regulatory mechanisms in dopaminergic neurons of the mesolimbic system. Proc Natl Acad Sci U S A 106:20081–20086. CrossRef Medline

Braff DL, Geyer MA, Swerdlow NR (2001) Human studies of prepulse inhibition of startle: normal subjects, patient groups, and pharmacological studies. Psychopharmacology (Berl) 156:234–258. CrossRef Medline

Brown AJ, Fisher DA, Kouranova E, McCoy A, Forbes K, Wu Y, Henry R, Ji D, Chambers A, Warren J, Shu W, Weinstein EJ, Cui X (2013) Whole-rat conditional gene knockout via genome editing. Nat Methods 10:638–640. CrossRef Medline

Budygin EA, Brodie MS, Sotnikova TD, Mateo Y, John CE, Cyr M, Gainetdinov RR, Jones SR (2004) Dissociation of rewarding and dopamine transporter-mediated properties of amphetamine. Proc Natl Acad Sci U S A 101:7781–7786. CrossRef Medline

Caffino L, Giannotti G, Mottarlini F, Racagni G, Fumagalli F (2017) Developmental exposure to cocaine dynamically dysregulates cortical Arc/ Arg3.1 modulation in response to a challenge. Neurotox Res 31:289–297. CrossRef Medline

Carbery ID, Ji D, Harrington A, Brown V, Weinstein EJ, Liaw L, Cui X (2010) Targeted genome modification in mice using zinc-finger nucleases. Genetics 186:451–459. CrossRef Medline

Carboni E, Spielewoy C, Vacca C, Nosten-Bertrand M, Giros B, Di Chiara G (2001) Cocaine and amphetamine increase extracellular dopamine in the nucleus accumbens of mice lacking the dopamine transporter gene. J Neurosci 21:RC141:1–4. Medline

Carlsson A (1987) Perspectives on the discovery of central monoaminergic neurotransmission. Annu Rev Neurosci 10:19–40. CrossRef Medline

Carlsson ML (2000) On the role of cortical glutamate in obsessive-compulsive disorder and attention-deficit hyperactivity disorder, two phenomenologically antithetical conditions. Acta Psychiatr Scand 102: 401–413. CrossRef Medline

Chen R, Tilley MR, Wei H, Zhou F, Zhou FM, Ching S, Quan N, Stephens RL, Hill ER, Nottoli T, Han DD, Gu HH (2006) Abolished cocaine reward in mice with a cocaine-insensitive dopamine transporter. Proc Natl Acad Sci U S A 103:9333–9338. CrossRef Medline

Cyr M, Beaulieu JM, Laakso A, Sotnikova TD, Yao WD, Bohn LM, Gainetdinov RR, Caron MG (2003) Sustained elevation of extracellular dopamine causes motor dysfunction and selective degeneration of striatal GABAergic neurons. Proc Natl Acad Sci U S A 100:11035–11040. CrossRef Medline

Egan MF, Kojima M, Callicott JH, Goldberg TE, Kolachana BS, Bertolino A, Zaitsev E, Gold B, Goldman D, Dean M, Lu B, Weinberger DR (2003) The BDNF val66met polymorphism affects activity-dependent secretion of BDNF and human memory and hippocampal function. Cell 112:257–269. CrossRef Medline

Espinoza S, Lignani G, Caffino L, Maggi S, Sukhanov I, Leo D, Mus L, Emanuele M, Ronzitti G, Harmeier A, Medrihan L, Sotnikova TD, Chieregatti E, Hoener MC, Benfenati F, Tucci V, Fumagalli F, Gainetdinov RR (2015) TAAR1 modulates cortical glutamate NMDA receptor function. Neuropsychopharmacology 40:2217–2227. CrossRef Medline

Farné M (1970) Induced motion in three dimensions. Percept Mot Skills 30:426. CrossRef

Fields RD, Lee PR, Cohen JE (2005) Temporal integration of intracellular Ca^{2+} signaling networks in regulating gene expression by action potentials. Cell Calcium 37:433–442. CrossRef Medline

Flores P, Pellón R (1997) Effects of d-amphetamine on temporal distributions of schedule-induced polydipsia. Pharmacol Biochem Behav 57:81–87. CrossRef Medline

Frau R, Mosher LJ, Bini V, Pillolla G, Pes R, Saba P, Fanni S, Devoto P, Bortolato M (2016) The neurosteroidogenic enzyme 5α-reductase modulates the role of D1 dopamine receptors in rat sensorimotor gating. Psychoneuroendocrinology 63:59–67. CrossRef Medline

Fumagalli F, Gainetdinov RR, Valenzano KJ, Caron MG (1998) Role of do-

pamine transporter in methamphetamine-induced neurotoxicity: evidence from mice lacking the transporter. J Neurosci 18:4861–4869. Medline

Fumagalli F, Racagni G, Colombo E, Riva MA (2003) BDNF gene expression is reduced in the frontal cortex of dopamine transporter knockout mice. Mol Psychiatry 8:898–899. CrossRef Medline

Gainetdinov RR (2008) Dopamine transporter mutant mice in experimental neuropharmacology. Naunyn Schmiedebergs Arch Pharmacol 377: 301–313. CrossRef Medline

Gainetdinov RR, Caron MG (2000) An animal model of attention deficit hyperactivity disorder. Mol Med Today 6:43–44. CrossRef Medline

Gainetdinov RR, Caron MG (2001) Genetics of childhood disorders: XXIV. ADHD, part 8: hyperdopaminergic mice as an animal model of ADHD. J Am Acad Child Adolesc Psychiatry 40:380–382. CrossRef Medline

Gainetdinov RR, Wetsel WC, Jones SR, Levin ED, Jaber M, Caron MG (1999) Role of serotonin in the paradoxical calming effect of psychostimulants on hyperactivity. Science 283:397–401. CrossRef Medline

Gainetdinov RR, Mohn AR, Caron MG (2001) Genetic animal models: focus on schizophrenia. Trends Neurosci 24:527–533. CrossRef Medline

Gainetdinov RR, Bohn LM, Sotnikova TD, Cyr M, Laakso A, Macrae AD, Torres GE, Kim KM, Lefkowitz RJ, Caron MG, Premont RT (2003) Dopaminergic supersensitivity in G protein-coupled receptor kinase 6-deficient mice. Neuron 38:291–303. CrossRef Medline

Galloway EM, Woo NH, Lu B (2008) Chapter 15 Persistent neural activity in the prefrontal cortex: A mechanism by which BDNF regulates working memory? Prog Brain Res 169:251–266. CrossRef Medline

Gardoni F, Bellone C (2015) Modulation of the glutamatergic transmission by dopamine: a focus on Parkinson, Huntington and addiction diseases. Front Cell Neurosci 9:25. CrossRef Medline

Gaspar P, Bloch B, Le Moine C (1995) D1 and D2 receptor gene expression in the rat frontal cortex: cellular localization in different classes of efferent neurons. Eur J Neurosci 7:1050–1063. CrossRef Medline

Geurts AM, et al. (2009) Knockout rats produced using designed zinc finger nucleases. Science 325:433. CrossRef Medline

Giros B, Jaber M, Jones SR, Wightman RM, Caron MG (1996) Hyperlocomotion and indifference to cocaine and amphetamine in mice lacking the dopamine transporter. Nature 379:606–612. CrossRef Medline

Goldman-Rakic PS (1996) Regional and cellular fractionation of working memory. Proc Natl Acad Sci U S A 93:13473–13480. CrossRef Medline

Goldman-Rakic PS, Lidow MS, Smiley JF, Williams MS (1992) The anatomy of dopamine in monkey and human prefrontal cortex. J Neural Transm Suppl 36:163–177. Medline

Hansen FH, et al. (2014) Missense dopamine transporter mutations associate with adult parkinsonism and ADHD. J Clin Invest 124:3107–3120. CrossRef Medline

Howes OD, Kapur S (2009) The dopamine hypothesis of schizophrenia: version III–the final common pathway. Schizophr Bull 35:549–562. CrossRef Medline

Illiano P, Bass CE, Fichera L, Mus L, Budygin EA, Sotnikova TD, Leo D, Espinoza S, Gainetdinov RR (2017) Recombinant adeno-associated virus-mediated rescue of function in a mouse model of dopamine transporter deficiency syndrome. Sci Rep 7:46280. CrossRef Medline

Jaber M, Dumartin B, Sagné C, Haycock JW, Roubert C, Giros B, Bloch B, Caron MG (1999) Differential regulation of tyrosine hydroxylase in the basal ganglia of mice lacking the dopamine transporter. Eur J Neurosci 11:3499–3511. CrossRef Medline

John CE, Jones SR (2007) Voltammetric characterization of the effect of monoamine uptake inhibitors and releasers on dopamine and serotonin uptake in mouse caudate-putamen and substantia nigra slices. Neuropharmacology 52:1596–1605. CrossRef Medline

Jones SR, Gainetdinov RR, Jaber M, Giros B, Wightman RM, Caron MG (1998) Profound neuronal plasticity in response to inactivation of the dopamine transporter. Proc Natl Acad Sci U S A 95:4029–4034. CrossRef Medline

Jones SR, Mathews TA, Budygin EA (2006) Effect of moderate ethanol dose on dopamine uptake in rat nucleus accumbens in vivo. Synapse 60:251–255. CrossRef Medline

Kahlig KM, Lute BJ, Wei Y, Loland CJ, Gether U, Javitch JA, Galli A (2006) Regulation of dopamine transporter trafficking by intracellular amphetamine. Mol Pharmacol 70:542–548. CrossRef Medline

Kawagoe KT, Zimmerman JB, Wightman RM (1993) Principles of voltam-

metry and microelectrode surface states. J Neurosci Methods 48:225–240. CrossRef Medline

Kesner RP, Rogers J (2004) An analysis of independence and interactions of brain substrates that subserve multiple attributes, memory systems, and underlying processes. Neurobiol Learn Mem 82:199–215. CrossRef Medline

Kuhr WG, Wightman RM (1986) Real-time measurement of dopamine release in rat brain. Brain Res 381:168–171. CrossRef Medline

Kurian MA, Li Y, Zhen J, Meyer E, Hai N, Jürgen Christen-H, Hoffmann GF, Jardine P, von Moers A, Mordekar SR, O'Callaghan F, Wassmer E, Wraige E, Dietrich C, Lewis T, Hyland K, Heales SJR, Sanger T, Gissen P, Assmann BE, et al. (2011) Clinical and molecular characterisation of hereditary dopamine transporter deficiency syndrome: an observational cohort and experimental study. Lancet Neurol 10:54–62. CrossRef Medline

Kurian MA, Zhen J, Cheng SY, Li Y, Mordekar SR, Jardine P, Morgan NV, Meyer E, Tee L, Pasha S, Wassmer E, Heales SJ, Gissen P, Reith ME, Maher ER (2009) Homozygous loss-of-function mutations in the gene encoding the dopamine transporter are associated with infantile parkinsonism-dystonia. J Clin Invest 119:1595–1603. CrossRef Medline

Leo D, Mus L, Espinoza S, Hoener MC, Sotnikova TD, Gainetdinov RR (2014) Taar1-mediated modulation of presynaptic dopaminergic neurotransmission: role of D2 dopamine autoreceptors. Neuropharmacology 81:283–291. CrossRef Medline

Lidow MS, Goldman-Rakic PS, Gallager DW, Rakic P (1991) Distribution of dopaminergic receptors in the primate cerebral cortex: quantitative autoradiographic analysis using [3H]raclopride, [3H]spiperone and [3H]SCH23390. Neuroscience 40:657–671. CrossRef Medline

Moreno M, Flores P (2012) Schedule-induced polydipsia as a model of compulsive behavior: neuropharmacological and neuroendocrine bases. Psychopharmacology (Berl) 219:647–659. CrossRef Medline

Morice E, Denis C, Giros B, Nosten-Bertrand M (2004) Phenotypic expression of the targeted null-mutation in the dopamine transporter gene varies as a function of the genetic background. Eur J Neurosci 20:120–126. CrossRef Medline

Ng J, et al. (2014) Dopamine transporter deficiency syndrome: phenotypic spectrum from infancy to adulthood. Brain 137:1107–1119. CrossRef Medline

Paxinos G, Watson C (2005) The rat brain in stereotaxic coordinates, Ed 5. San Diego: Elsevier Academic.

Pruunsild P, Sepp M, Orav E, Koppel I, Timmusk T (2011) Identification of cis-Elements and Transcription Factors Regulating Neuronal Activity-Dependent Transcription of Human BDNF Gene. J Neurosci 31:3295–3308. CrossRef Medline

Ralph RJ, Paulus MP, Fumagalli F, Caron MG, Geyer MA (2001) Prepulse inhibition deficits and perseverative motor patterns in dopamine transporter knock-out mice: differential effects of D1 and D2 receptor antagonists. J Neurosci 21:305–313. Medline

Revel FG, Moreau JL, Gainetdinov RR, Bradaia A, Sotnikova TD, Mory R, Durkin S, Zbinden KG, Norcross R, Meyer CA, Metzler V, Chaboz S, Ozmen L, Trube G, Pouzet B, Bettler B, Caron MG, Wettstein JG, Hoener MC (2011) TAAR1 activation modulates monoaminergic neurotransmission, preventing hyperdopaminergic and hypoglutamatergic activity. Proc Natl Acad Sci U S A 108:8485–8490. CrossRef Medline

Revel FG, Moreau JL, Gainetdinov RR, Ferragud A, Velázquez-Sánchez C, Sotnikova TD, Morairty SR, Harmeier A, Groebke Zbinden K, Norcross RD, Bradaia A, Kilduff TS, Biemans B, Pouzet B, Caron MG, Canales JJ, Wallace TL, Wettstein JG, Hoener MC (2012) Trace amine-associated receptor 1 partial agonism reveals novel paradigm for neuropsychiatric therapeutics. Biol Psychiatry 72:934–942. CrossRef Medline

Rocha BA, Fumagalli F, Gainetdinov RR, Jones SR, Ator R, Giros B, Miller GW, Caron MG (1998) Cocaine self-administration in dopamine-transporter knockout mice. Nat Neurosci 1:132–137. CrossRef Medline

Sanger DJ (1977) d-amphetamine and adjunctive drinking in rats. Psychopharmacology (Berl) 54:273–276. CrossRef Medline

Saunders C, Ferrer JV, Shi L, Chen J, Merrill G, Lamb ME, Leeb-Lundberg LM, Carvelli L, Javitch JA, Galli A (2000) Amphetamine-induced loss of human dopamine transporter activity: an internalization-dependent and cocaine-sensitive mechanism. Proc Natl Acad Sci U S A 97:6850–6855. CrossRef Medline

Siciliano CA, Fordahl SC, Jones SR (2016) Cocaine self-administration produces long-lasting alterations in dopamine transporter responses to cocaine. J Neurosci 36:7807–7816. CrossRef Medline

Sora I, Wichems C, Takahashi N, Li XF, Zeng Z, Revay R, Lesch KP, Murphy DL, Uhl GR (1998) Cocaine reward models: conditioned place preference can be established in dopamine- and in serotonin-transporter knockout mice. Proc Natl Acad Sci U S A 95:7699–7704. CrossRef Medline

Sotnikova TD, Beaulieu JM, Barak LS, Wetsel WC, Caron MG, Gainetdinov RR (2005) Dopamine-independent locomotor actions of amphetamines in a novel acute mouse model of Parkinson disease. PLOS Biol 3:e271. CrossRef Medline

Spielewoy C, Roubert C, Hamon M, Nosten-Bertrand M, Betancur C, Giros B (2000) Behavioural disturbances associated with hyperdopaminergia in dopamine-transporter knockout mice. Behav Pharmacol 11:279–290. CrossRef Medline

Sun X, Lin Y (2016) Npas4: Linking Neuronal Activity to Memory. Trends Neurosci 39:264–275. CrossRef Medline

Sukhanov I, Espinoza S, Yakovlev DS, Hoener MC, Sotnikova TD, Gainetdinov RR (2014) TAAR1-dependent effects of apomorphine in mice. Int J Neuropsychopharmacol 17:1683–1693. CrossRef Medline

Swerdlow NR, Geyer MA, Braff DL (2001) Neural circuit regulation of prepulse inhibition of startle in the rat: current knowledge and future challenges. Psychopharmacology (Berl) 156:194–215. CrossRef Medline

Thomsen M, Han DD, Gu HH, Caine SB (2009) Lack of cocaine self-administration in mice expressing a cocaine-insensitive dopamine transporter. J Pharmacol Exp Ther 331:204–211. CrossRef Medline

Vaughan RA, Foster JD (2013) Mechanisms of dopamine transporter regulation in normal and disease states. Trends Pharmacol Sci 34:489–496. CrossRef Medline

Vecchio LM, Bermejo MK, Beerepoot P, Ramsey AJ, Salahpour A (2014) N-terminal tagging of the dopamine transporter impairs protein expression and trafficking in vivo. Mol Cell Neurosci 61:123–132. CrossRef Medline

Vengeliene V, Bespalov A, Roßmanith M, Horschitz S, Berger S, Relo AL, Noori HR, Schneider P, Enkel T, Bartsch D, Schneider M, Behl B, Hansson AC, Schloss P, Spanagel R (2017) Towards trans-diagnostic mechanisms in psychiatry: neurobehavioral profile of rats with a loss-of-function point mutation in the dopamine transporter gene. Dis Model Mech 10:451–461. CrossRef Medline

Wheeler DS, Underhill SM, Stolz DB, Murdoch GH, Thiels E, Romero G, Amara SG (2015) Amphetamine activates rho GTPase signaling to mediate dopamine transporter internalization and acute behavioral effects of amphetamine. Proc Natl Acad Sci U S A 112:E7138–E7147. CrossRef Medline

Wong P, Chang CC, Marx CE, Caron MG, Wetsel WC, Zhang X (2012) Pregnenolone rescues schizophrenia-like behavior in dopamine transporter knockout mice. PLoS One 7:e51455. CrossRef Medline

Wong P, Sze Y, Chang CC, Lee J, Zhang X (2015) Pregnenolone sulfate normalizes schizophrenia-like behaviors in dopamine transporter knockout mice through the AKT/GSK3β pathway. Transl Psychiatry 5:e528. CrossRef Medline

Yamashita M, Fukushima S, Shen HW, Hall FS, Uhl GR, Numachi Y, Kobayashi H, Sora I (2006) Norepinephrine transporter blockade can normalize the prepulse inhibition deficits found in dopamine transporter knockout mice. Neuropsychopharmacology 31:2132–2139. CrossRef Medline

Yao WD, Gainetdinov RR, Arbuckle MI, Sotnikova TD, Cyr M, Beaulieu JM, Torres GE, Grant SG, Caron MG (2004) Identification of PSD-95 as a regulator of dopamine-mediated synaptic and behavioral plasticity. Neuron 41:625–638. CrossRef Medline

Yildiz Y, Pektas E, Tokatli A, Haliloglu G (2017) Hereditary dopamine transporter deficiency syndrome: challenges in diagnosis and treatment. Neuropediatrics 48:49–52. CrossRef Medline

Yorgason JT, España RA, Jones SR (2011) Demon voltammetry and analysis software: analysis of cocaine-induced alterations in dopamine signaling using multiple kinetic measures. J Neurosci Methods 202:158–164. CrossRef Medline

Young KA, Thompson PM, Cruz DA, Williamson DE, Selemon LD (2015) BA11 FKBP5 expression levels correlate with dendritic spine density in postmortem PTSD and controls. Neurobiol Stress 2:67–72. CrossRef Medline

Zheng F, Zhou X, Luo Y, Xiao H, Wayman G, Wang H (2011) Regulation of Brain-Derived Neurotrophic Factor Exon IV Transcription through Calcium Responsive Elements in Cortical Neurons (Amédée T, ed). PLoS ONE 6:e28441. CrossRef Medline